รายงานวิจัยฉบับสมบูรณ์

โครงการ การวิเคราะห์ประสิทธิภาพของเปลือกอาคารเพื่อการอนุรักษ์พลังงานในอาคาร กรณีศึกษาอาคารเรียนรวม มหาวิทยาลัยชินวัตร

โดย ผศ.ดร. อภิชาต ประดิษฐสมานนท์ และคณะ

พฤษภาคม 2550

สัญญาเลขที่ MRG4880159

รายงานวิจัยฉบับสมบูรณ์

โครงการ การวิเคราะห์ประสิทธิภาพของเปลือกอาคารเพื่อการอนุรักษ์พลังงานในอาคาร: กรณีศึกษาอาคารเรียนรวม มหาวิทยาลัยชินวัตร

คณะผู้วิจัย	สังกัด
1. ผศ.ดร. อภิชาต ประดิษฐสมานนท์	มหาวิทยาลัยชินวัตร
2. รศ.ดร. ศุภชาติ จงไพบูลย์พัฒนะ	สถาบันเทคโนโลยีนานาชาติสิรินธร มหาวิทยาลัยธรรมศาสตร์

สนับสนุนโดยสำนักงานคณะกรรมการการอุดมศึกษา และสำนักงานกองทุนสนับสนุนการวิจัย

(ความเห็นในรายงานนี้เป็นของผู้วิจัย สกอ. และ สกว. ไม่จำเป็นต้องเห็นด้วยเสมอไป)

กิตติกรรมประกาศ

รายงานการวิจัยเรื่อง **"การวิเคราะห์ประสิทธิภาพของเปลือกอาคารเพื่อการอนุรักษ์พลังงานในอาคาร: กรณีศึกษาอาคารเรียนรวม มหาวิทยาลัยชินวัตร"** เป็นโครงการที่จัดทำขึ้นโดยได้รับการสนับสนุนจากทุนพัฒนาศักยภาพในการทำงานวิจัยของอาจารย์รุ่นใหม่ ที่สำนักงานกองทุนสนับสนุนการวิจัย ได้ร่วมกับสำนักงานคณะกรรมการการศึกษา เพื่อสนับสนุนอาจารย์รุ่นใหม่ให้ทำวิจัยได้อย่างต่อเนื่อง

ผู้วิจัยขอขอบพระคุณ รองศาสตราจารย์ ดร. ศุภชาติ จงไพบูลย์พัฒนะ นักวิจัยที่ปรึกษา ที่ได้กรุณาสละเวลาให้คำปรึกษา ข้อเสนอแนะที่เป็นประโยชน์ยิ่งต่อการวิจัย และได้ให้ความช่วยเหลือจนกระทั่งงานวิจัยสำเร็จลุล่วงไปได้ด้วยดี ขอขอบพระคุณ Prof. Dr. Francisco Arumi-Noe ที่กรุณาให้คำปรึกษาและชี้แนะแนวทางในการจำลองสภาพโดยโปรแกรมคอมพิวเตอร์ นอกจากนี้ขอขอบคุณ ดร. ทรงเกียรติ มธุพยนต์ สำหรับคำแนะนำและความช่วยเหลือในการตรวจสอบข้อมูลการวิเคราะห์และประเมินราคาโครงสร้างอาคาร และคุณเกชา ธีระโกเมน ที่กรุณาให้ข้อมูลในการประเมินราคาระบบปรับอากาศ

สุดท้ายนี้ ขอขอบคุณสำนักงานกองทุนสนับสนุนการวิจัย และมหาวิทยาลัยชินวัตรที่สนับสนุนงบประมาณวิจัยเป็นค่าใช้จ่ายของโครงการวิจัยนี้

บทคัดย่อ

รหัสโครงการ: MRG4880159

ชื่อโครงการ: การวิเคราะห์ประสิทธิภาพของเปลือกอาคารเพื่อการอนุรักษ์พลังงานในอาคาร: กรณีศึกษาอาคารเรียนรวม มหาวิทยาลัยชินวัตร

ชื่อนักวิจัย: ผศ.ดร. อภิชาต ประดิษฐสมานนท์ มหาวิทยาลัยชินวัตร

ชื่อนักวิจัยที่ปรึกษา: รศ.ดร. ศุภชาติ จงไพบูลย์พัฒนะ สถาบันเทคโนโลยีนานาชาติสิรินธร มหาวิทยาลัยธรรมศาสตร์

E-mail Address: apichat@shinawatra.ac.th และ supachar@siit.tu.ac.th

ระยะเวลาโครงการ: 1 มิถุนายน 2548 ถึง 31 พฤษภาคม 2550

เปลือกอาคารของอาคารเรียนรวม มหาวิทยาลัยชินวัตรได้รับการออกแบบให้มีคุณสมบัติในการป้องกันความร้อนและความชื้นได้เป็นอย่างดี จากการคำนวณพบว่าอาคารเรียนรวมมีประสิทธิภาพในด้านการป้องกันการถ่ายเทความร้อนผ่านเปลือกอาคารดีกว่าค่ามาตรฐานภายในประเทศประมาณ 4 เท่า โดยมีค่าสัมประสิทธิ์การถ่ายเทความร้อนผ่านเปลือกอาคาร (Overall Thermal Transfer Value) เท่ากับ 10.16 W/m^2 การศึกษาครั้งนี้มีวัตถุประสงค์เพื่อศึกษาประสิทธิภาพของเปลือกอาคารของอาคารเรียนรวม มหาวิทยาลัยชินวัตร โดยใช้ข้อมูลทั้งการวัดจากสภาพอาคารจริงและการจำลองสภาพโดยโปรแกรมคอมพิวเตอร์ ข้อมูลจากการวัดค่าอุณหภูมิอากาศ ค่าอุณหภูมิผิวของผนังทึบและหน้าต่างกระจก รวมทั้งค่าความชื้นสัมพัทธ์ ทั้งภายนอกและภายในอาคาร และข้อมูลทางด้านอุตุนิยมวิทยาสำหรับค่าปริมาณแสงตรงและแสงกระจายของดวงอาทิตย์ ได้ถูกนำไปใช้ในการจำลองสภาพ เพื่อคำนวณค่าพลังงานความร้อนผ่านเปลือกอาคารใน 8 ทิศทาง ซึ่งจากผลการศึกษา พบว่าค่าเฉลี่ยพลังงานความร้อนผ่านเปลือกอาคารจริงแตกต่างจากค่าสัมประสิทธิ์การถ่ายเทความร้อนผ่านเปลือกอาคารจากการคำนวณเพียง 7% นอกจากนี้เมื่อทำการจำลองสภาพโดยใช้ข้อมูลสภาพแวดล้อมภายนอกจากการวัดในการคำนวณค่าพลังงานความร้อนผ่านวัสดุเปลือกอาคารทั่วไป พบว่าเปลือกอาคารของอาคารเรียนรวมมีประสิทธิภาพในการป้องกันการถ่ายเทความร้อนสูงกว่าวัสดุเปลือกอาคารทั่วไปอย่างชัดเจน แต่การใช้เปลือกอาคารที่มีน้ำหนักเบาและมีประสิทธิภาพสูงนี้ ก็มีผลทำให้มูลค่าการลงทุนของเปลือกอาคารสูงตามไปด้วย อย่างไรก็ตาม ผลจากการประเมินความคุ้มค่าเบื้องต้นพบว่าเปลือกอาคารชนิดนี้ นอกจากจะช่วยประหยัดพลังงานในการปรับอากาศอาคารแล้ว ยังช่วยลดค่าใช้จ่ายในด้านการลงทุนและการดำเนินการของระบบปรับอากาศและระบบโครงสร้างของอาคารอีกด้วย ทำให้ระยะเวลาคืนทุนอยู่ในช่วงประมาณ 3-5 ปี ขึ้นอยู่กับชนิดของวัสดุเปลือกอาคารทั่วไปที่นำมาเปรียบเทียบ นอกจากนี้ หากนำเปลือกอาคารที่มีประสิทธิภาพนี้ไปใช้กับอาคารทั่วไปโดยเฉพาะอาคารสูงในเขตเมือง จะช่วยให้สามารถประหยัดพลังงานและค่าใช้จ่ายได้ในสัดส่วนที่มากขึ้น และมีระยะเวลาคืนทุนที่สั้นลง

คำสำคัญ

เปลือกอาคาร, ค่าสัมประสิทธิ์การถ่ายเทความร้อนผ่านเปลือกอาคาร, การถ่ายเทความร้อน, ผนังฉนวนกันความร้อนภายนอก, กระจกฮีตสต๊อบ

Abstract

Project Code: MRG4880159

Project Title: Performance Analysis of the Building Envelope: A case study of the Main Hall, Shinawatra University

Investigators: Asst. Prof. Dr. Apichat Praditsmanont, Shinawatra University

Mentor: Assoc. Prof. Dr. Supachart Chungpaibulpatana, Sirindhorn International Institute of Technology, Thammasat University

E-mail Address: apichat@shinawatra.ac.th และ supachar@siit.tu.ac.th

Project Period: June 1, 2005 – May 31, 2007

The envelope of the Main Hall, Shinawatra University has been designed to provide a good protection from energy gain. According to the estimation, the Main Hall could achieve an OTTV (Overall Thermal Transfer Value) of 10.16 W/m^2, which is 4 times lower than the national standard. This study aims to evaluate the actual energy performance of the Main Hall's building envelope using field measurements and simulations. The air temperatures and surface temperatures as well as the relative humidity were measured both indoors and outdoors. An hourly average meteorological data for insolations were utilized in order to calculate the solar gain by light transmission. Based on the empirical data, the energy fluxes through the envelope on 8 different orientations were simulated and the average value was found within 7% of the estimated OTTV. Using the same empirical data for the outdoor condition, the simulations for other common types of building envelope were carried out for comparisons. The results of the analysis show that the Main Hall's building envelope outperforms other envelope types in preventing energy transfer into the building. Although the use of the lightweight and highly energy efficient envelope helps reduce the operating and investment costs of the air conditioning system as well as the cost of building structure, it also increases the investment cost of the envelope substantially. However the preliminary investigation reveals that the investment cost of the Main Hall's envelope requires a simple pay back period of about 3-5 years depending on envelope types used in the comparison. Furthermore, it should be noted that greater saving and more favorable pay back period should be obtained if this high energy efficient envelope is applied to other typical buildings, especially those high-rise structures in urban areas.

Keywords

Building Envelope, Overall Thermal Transfer Value, OTTV, Heat Transfer, External Insulation and Finished System, Heat-stop glass

Performance Analysis of the Building Envelope:

A case study of the Main Hall, Shinawatra University

Apichat Praditsmanont[1]* and Supachart Chungpaibulpatana[2]

[1]*School of Technology, Shinawatra University*

99 Moo 10 Bangtoey, Samkok, Pathumthani 12160, Thailand

[2]*Sirindhorn International Institute of Technology, Thammasat University - Rangsit Campus*

P.O.Box 22, Pathum Thani 12121, Thailand

Introduction

The Main Hall of Shinawatra University is located in the rural area of Pathumthani province and surrounded by several trees, plants, 4 large pools, and 2 lakes, which creates cool and comfort natural environment around campus. This 5-storey building has a circular shape with a central atrium and a dome skylight. Its front elevation and section are shown in Figure 1. The building has 21,810 m^2 of the floor area. The building height is 42 meters and its diameter is approximately 73 meters. The Main Hall is a center for teaching and learning. Offices of university executives and administrative departments are located on the 1^{st} and 2^{nd} floors of the building. The 3^{rd} floor houses several classrooms and computer laboratories. Two main auditoriums, large classrooms, library, and offices of faculty members are on the 4^{th} and 5^{th} floors.

The Main Hall of Shinawatra University has been designed with true understanding of the hot-humid climate in Thailand and a consideration of better quality of life for its occupants. Several design strategies are implemented in an attempt to minimize the energy gain, moisture penetration, and air infiltration.

The use of the circular shape reduces the external surface area of the building, as well as the surface to floor area ratio, and minimizes heat gain through the envelope. The circular shape also helps decrease the pressure difference between the windward and leeward sides. It allows wind to flow through the building much smoother than normal rectangular buildings. Thus, air infiltration and leakage is reduced. Stacking a larger upper floor on top of the lower floor creates an inverted cascading shape, which shades the lower floor from direct solar radiation. Horizontal shading devices are also installed on some parts of the building envelope [1]

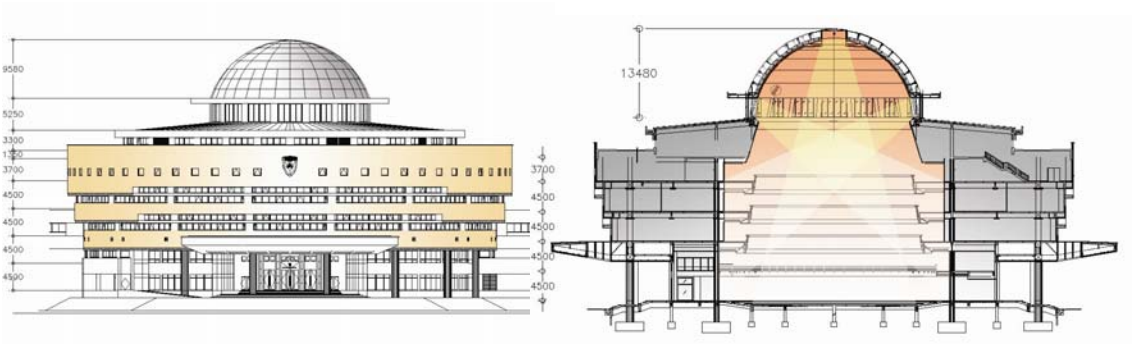

Figure 1 Front elevation and section of the Main Hall

The Main Hall's envelope provides a good protection from energy gain and moisture penetration. It consists of approximately 3,843 m^2 of opaque wall areas and 1,805 m^2 of window areas. The External Insulation and Finished System (EIFS) has been selected as an opaque wall system. This light-weight wall system has high resistance due to the use of 3-inch fire retardant Expanded Polystyrene (EPS) insulator board [2]. The windows and openings of the Main Hall have been installed with the heat-stop glass. This double-glazed glass has low Shading Coefficient (SC), low conductivity (U-value), and low moisture penetration. Table 1 shows the physical properties of the EIFS and heat-stop glass, and Figure 2 shows sectional details of the EIFS and heat-stop glass.

Type	Thickness (mm)	Weight (kg/m^2)	U-value (W/m^2 K)	Shading Coefficient (SC)	Light Transmission (LT)	LT/SC Ratio
EIFS	300	36	0.23	-	-	-
Heat-stop	28	65	1.80	0.27	50%	1.85

Table 1 Physical Properties of External Insulation and Finished System (EIFS) and Heat-stop Glass

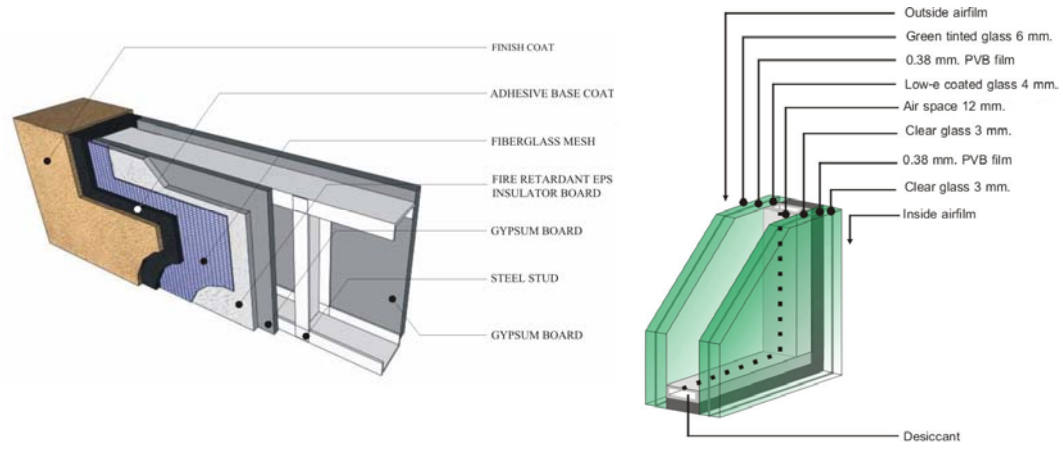

Figure 2 Sectional details of External Insulation and Finished System (EIFS) and heat-stop glass.

According to the estimation of the OTTVEE (Overall Thermal Transfer and Energy Estimation) program, the Main Hall could achieve OTTV (Overall Thermal Transfer Value) and RTTV (Roof Thermal Transfer Value) of 10.16 and 5.91 W/m^2 respectively, which are about 4 times lower than those recommended in the Thai national standard for old and new buildings as illustrated in Figure 3 [2].

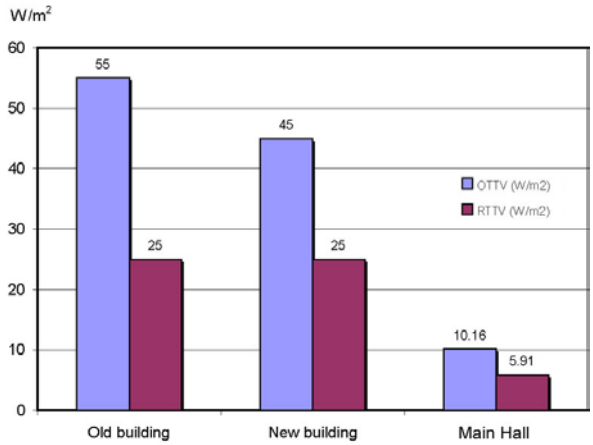

Figure 3 Comparisons between OTTV and RTTV of the Main Hall and other buildings.

Since the Main Hall has been operating for more than 5 years, the building has not been assessed in term of its energy performance. It will be invaluable to discover the effects of the envelope design strategies implemented in this building on the energy gain, moisture penetration and energy use.

Objective

This study aims to evaluate the actual energy performance of the Main Hall's building envelope using both on-site field measurements [3][4] and simulations. The main objectives are:

- To evaluate the ability of the envelope in preventing energy gain and moisture penetration
- To simulate the energy flux through the envelope based on the empirical data and compare it with the estimated OTTV
- To compare the investment cost of the envelope of the Main Hall with other regular building envelop systems as well as the investment and operating costs of the air conditioning and other building systems

The finding of this study should be beneficial to the improvement of the Main Hall. It could also be utilized in the design of new buildings and the improvement of existing buildings in the conservation of energy.

Method

Field Measurement

The on-site field measurement is intended to collect the empirical data necessary for the calculation of the actual OTTV value. The collected data of both indoors and outdoors include air temperatures, surface temperatures of the EIFS and heat-stop glass, and the relative humidity. An hourly average meteorological data for insolations are also acquired [5][6][7][8]. In addition, these data can be used in the simulation of other typical building envelope types so that the comparisons with the Main Hall's envelope in term of the energy cost saving can be carried out. Consequently, the actual performance of the Main Hall's envelope can be assessed.

The data loggers and sensors are installed on the 4th floor of the Main Hall in 8 orientations of the envelope as shown in Figure 4 as north, northeast, east, southeast, south, southwest, west, and northwest directions. Air temperatures and surface temperatures of the EIFS and heat stop glass as well as the humidity ratios are measured both indoors and outdoors. Before collecting the data, the Main Hall and its operation is shut down for 24 hours in order to stabilize the building to the passive state after a normal operation. The data are collected every 15 minutes continuously. During the semester break (March-May and October), all collected data can be used while only data collected during the weekend is used during the regular semester.

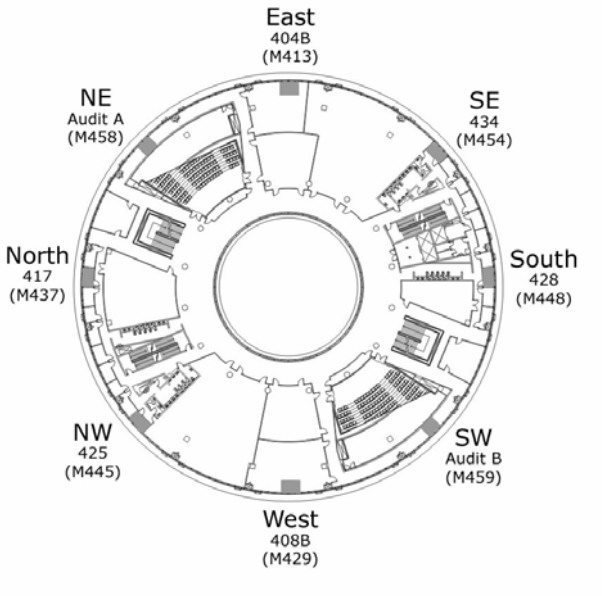

Figure 4 Location of dataloggers on the 4th floor of the Main Hall.

Using this empirical data together with the hourly average meteorological data for insolations, the OTTV through the envelope can be calculated for each orientation and for the overall envelope area. The typical expression of OTTV is as follows [9][10][11]:

$$OTTV_i = ((1\text{-}WWR))\times U_w \times TD_{eg}) + (WWR \times U_g \times DT) + (WWR \times SC \times SHGC \times ESR) \quad (1)$$

where $OTTV_i$ = OTTV of a wall with the same material and orientation (W/m^2)

WWR = window to overall wall area ratio

U_w = thermal conductance or U-value of an opaque wall (W/m^2 K)

TD_{eg} = equivalent temperature difference of an opaque wall (K)

U_g = thermal conductance of glazing (W/m^2 K)

DT = temperature difference of glazing window (K)

SC = shading coefficient of shading device

$SHGC$ = solar heat gain coefficient of glazing

ESR = effective solar radiation (W/m^2)

To calculate the value of OTTV based on the empirical and simulated data, TD_{eg} and DT are replaced by the temperature difference between the outdoor and indoor surface of the EIFS, and that of the heat-stop window, respectively.

The product of SHGC and ESR is substituted by the solar gain by light transmission (G_t) through the heat-stop window, which is the product of the solar incident radiation (I) and the solar admittance by transmission (a_t).

$$G_t = I \times a_t \quad (2)$$

In order to calculate the solar radiation incident (I) on the window, the position of the sun, the orientation of the window, and the values of solar radiation must be obtained. The hourly average values of the direct normal radiation (I_{DN}), sky diffuse (I_{SKY}), and global horizontal or ground radiation (I_{GND}) are provided by the meteorological data [5][6][7][8]. The direct normal radiation is the intensity of the direct normal solar beam measured on a plane perpendicular to the solar ray. The sky diffuse is the diffused sky radiation on a horizontal plane and the ground radiation is the sum of the sky diffuse and direct radiation on a horizontal plane.

The position of the sun is described in the solar coordinates, which can be calculated based on the altitude and azimuth angles. The altitude angle is measured from the horizon toward

the zenith following the arc of the great circle that goes through the sun. The azimuth angle is measured along the ground from the south toward the east.

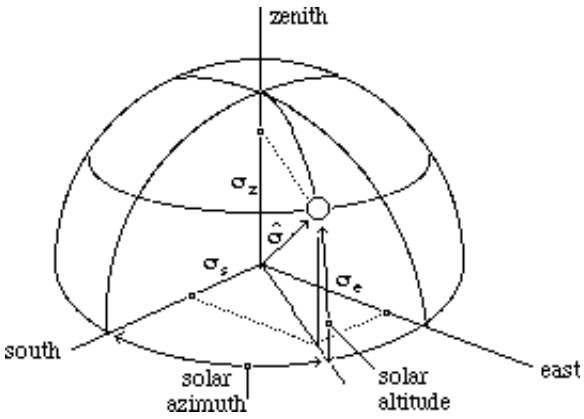

Figure 5 Solar position described by the solar angles and by the direction cosines

The solar coordinates are represented with the position vector "$\hat{\sigma}$", which are the projections of the solar position along the south (σ_S), east (σ_E), and zenith (σ_Z) axis as shown in Figure 5. The relation between σ and the altitude and azimuth angles are:

$$\sigma_S = \cos(altitude)\cos(azimuth) \quad \sigma_E = \cos(altitude)\sin(azimuth) \quad \sigma_Z = \sin(altitude)$$
$$\sigma_S^2 + \sigma_E^2 + \sigma_Z^2 = 1 \tag{3}$$

The orientation of the window is defined by specifying the unit vector normal to the window surface, which requires two angles, the zenith and azimuth. The zenith angle measures the aperture distance from the zenith axis, and the azimuth angle measures the aperture distance on the ground relative to the south direction. The south, east and zenith components of the unit vector normal to the surface are given by

$$n_S = \sin(zenith)\cos(azimuth)$$
$$n_E = \sin(zenith)\sin(azimuth)$$
$$n_Z = \cos(zenith) \tag{4}$$

The solar radiation incident on the window consists of 2 parts which are the direct insolation (I_d) and the diffuse radiation. The direct insolation can be calculated by multiplying the projected area (or relative insolation) and the direct normal radiation (I_{DN}). The fraction of the surface area projected onto the solar beam is given by the "dot" product, and the result is also the cosine of the angle of incidence (ϕ).

$$\hat{\sigma} \cdot \hat{n} = \sigma_S n_S + \sigma_E n_E + \sigma_Z n_Z \qquad \hat{\sigma} \cdot \hat{n} = \cos(\phi) \tag{5}$$

$$\text{Direct Insolation}(I_d) = (\hat{\sigma} \cdot \hat{n}) \times I_{DN} \tag{6}$$

The diffuse radiation comes from the sky and the ground reflection. Each contribution is determined by the respective view factor. The sky diffuse radiation (I_s) is the product of the sky view and the sky diffuse (I_{SKY}), and the ground reflection (I_g) is the product of the ground view and the global horizontal radiation (I_{GND}) times the average reflectance of the ground.

$$\text{sky view} = \frac{1+\cos(zenith)}{2} \qquad \text{ground view} = \frac{1-\cos(zenith)}{2} \tag{7}$$

$$\text{Sky Diffuse}(I_s) = \text{sky view} \times I_{SKY} \tag{8}$$

$$\text{Ground Reflection}(I_g) = \text{ground view} \times \text{ground reflectance} \times I_{GND} \tag{9}$$

According to Equation (2), the solar gain by transmission (G_t) is the product of the incident radiation (I) times the admittance by transmission factor (a_t). The solar admittance by transmission (a_t) depends on the transmittance coefficient of the glass (τ), the exposure of the window (e), and on the cavity absorptance (α) of the space behind the window, which is assumed to be 100% in this case.

$$a_t = e\tau\alpha \tag{10}$$

In general, the admittance factor is different for each of the three radiant sources because the transmittance and absorptance coefficients vary according to the angle of incidence. The exposures of the window to different radiant sources are also different. Therefore, the expression for the solar gain by transmission (G_t) from three separated radiant sources is given as follows:

$$G_t = \underbrace{a_d e_d I_d}_{direct} + \underbrace{a_s e_s I_s}_{sky} + \underbrace{a_g e_g I_g}_{ground} \tag{11}$$

Because of the overhangs of the Main Hall protecting the heat-stop windows from the solar radiation, the exposure of the direct insolation (e_d) incident on the windows is reduced significantly with the average of 74% reduction over all orientations. In addition, the exposure of the sky diffuse (e_s) decreases from 0.5 to 0.25, which in turn reduces the sky diffuse radiation to 50%, while the exposure of the ground reflection remains at 0.5.

Simulation

Using the same empirical data for the outdoor condition, the simulations for both EIFS, and other common types of building envelope including 10 cm. brick and 20 cm. concrete walls both with and without 7.5 cm external insulation are carried out for comparisons. For each material, simulations are carried out under 2 different conditions. One is a passive condition in which there is no air conditioning. This condition is similar to the condition of

the field measurement. The temperatures and energy fluxes inside the material are simulated and compared with the data from the field measurement in order to verify their validity and reliability. The other is an active condition. In this condition, it is similar to turning on the air conditioning in order to keep the indoor surface temperature of the material at a constant temperature of 25.5C. In addition to the simulated temperatures and energy fluxes inside the material, the heat removals by the air conditioning system can also be calculated and compared. These simulated results under the active condition can be used to estimate the investment and operating costs of the air conditioning system.

To illustrate the theoretical basis used in the simulation, the mathematical model of the simulation is described briefly [12][13][14]. A wall composes of a series of slabs. Each slab is made of a uniform material of a given thickness "L" and is divided into several layers of equal thickness. A node is placed at the center of each layer to monitor the temperature and energy flux inside the wall. Figure 6 shows a composite wall of 3 slabs and a series of node in the layers.

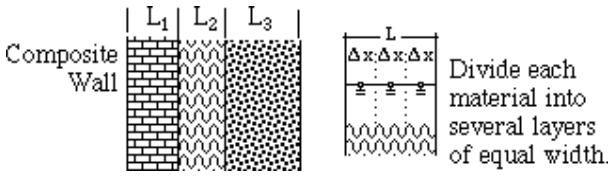

Figure 6 Sample composite wall of 3 slabs and a series of node in the layers.

To calculate the dynamic temperature inside the wall, the heat diffusion equation is used in the simulation. By integrating the heat diffusion equation in differential form over a volume of a layer "τ", Equation (12) is obtained.

$$\rho c \frac{\partial T}{\partial t} = \nabla \cdot \underline{q} + h \quad \Rightarrow \quad \int_{\tau} \rho c \frac{\partial T}{\partial t} d\tau = \oint_{A} \underline{q} \cdot d\underline{A} + \int_{\tau} h d\tau \tag{12}$$

Simplified assumptions are made that each layer contains single material, heat flows only in one direction from surface to surface, and all the mass is concentrated at a single node in the center of the layer. The heat diffusion equation can be written as a typical electronic resistance-capacitance (RC) format as shown in Figure 7.

$$C \frac{dT_o}{dt} = K(T_1 - T_o) + K(T_2 - T_o) + H \tag{13}$$

where $C = \rho c A \Delta x$ $K = \frac{2kA}{\Delta x}$ $H = A\int_{x_1}^{x_2} h dx$

ρ	=	mass density	c	=	specific heat capacitance
A	=	frontal area	k	=	heat conductivity
h	=	heat source	x	=	position from left to right

"*C*" is referred to as the heat capacitance of the node while "*K*" is the heat transfer coefficient of half a layer. "*H*" represents the heat absorbed by the node.

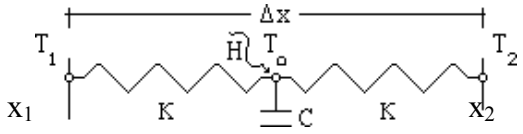

Figure 7 Typical layer arrangement of RC diagram.

Equation (13) can also be expressed as follows:

$$\frac{dT_o}{dt} + \nu T_o = \nu D \tag{14}$$

where

$$\nu = \frac{2K}{C} \quad \text{relaxation rate}$$

$$D = \frac{T_1 + T_2}{2} + \frac{H}{2K} \quad \text{driving temperature}$$

"D" is referred to as the driving temperature of the node. "T_o" is referred to as the response temperature of the node. Equation (14) can be re-written by using the integration factor "$e^{\nu t}$"

$$\frac{d\left(T_o e^{\nu t}\right)}{dt} = \nu D e^{\nu t} \tag{15}$$

Noting that the identity "$\nu D e^{\nu t} = \frac{d\left(D e^{\nu t}\right)}{dt} - \frac{dD}{dt} e^{\nu t}$", this equation becomes:

$$\frac{d}{dt}\left(T_o e^{\nu t}\right) = \frac{d}{dt}\left(D e^{\nu t}\right) - \left(\frac{dD}{dt}\right) e^{\nu t} \tag{16}$$

When the values of the driving temperature at discrete time intervals are known, the equation can be written in the following forms.

$$\int_t^{t+\Delta t} \frac{d}{dt}\left(T_o e^{\nu t}\right) dt = \int_t^{t+\Delta t} \frac{d}{dt}\left(D e^{\nu t}\right) dt - \int_t^{t+\Delta t} \left(\frac{dD}{dt}\right) e^{\nu t} dt$$

$$T_o' e^{\nu(t+\Delta t)} - T_o e^{\nu t} = D' e^{\nu(t+\Delta t)} - D e^{\nu t} - \int_t^{t+\Delta t} \left(\frac{dD}{dt}\right) e^{\nu t} dt$$

The ”primed” quantities are the values at the new time ”t +Δt” and the ”unprimed” quantities are the values at the previous time ”t.” Since the values of the driving temperature at the beginning and at the end of the time interval are known but not in between, it is assumed that the values in between are a linear interpolation of the end values. Thus the time derivative is a constant: over the time interval i.e. $\frac{dD}{dt} = \frac{D' - D}{\Delta t}$ which means that it may be taken out of the integral in the last term of the right hand side of the equation above.

$$T_o' e^{\nu(t+\Delta t)} - T_o e^{\nu t} = D' e^{\nu(t+\Delta t)} - D e^{\nu t} - \left(\frac{D' - D}{\nu \Delta t}\right)\left(e^{\nu(t+\Delta t)} - e^{\nu t}\right)$$

If all the time intervals are assumed to be the same, then all of the ”t +Δt” terms are constants for the layer. These terms are collected as factors of the temperatures to obtain Equation (17).

$$T_o' = \left(\alpha T_o + \gamma D\right) + \beta D' \tag{17}$$

The constant factors are defined as:

$$\alpha = e^{-\nu \Delta t} \quad \gamma = \left(\frac{1-\alpha}{\nu \Delta t}\right) - \alpha \quad \beta = 1 - \left(\frac{1-\alpha}{\nu \Delta t}\right) \tag{18}$$

It is noted that the sum of these factors is equal to one; thus, this solution satisfies energy conservation. The term in parenthesis in Equation (17) contains temperatures from the previous instant in time. Their values are already known; therefore, the value of the term in parenthesis is also known. Equation (17) can be expressed in a simpler form.

$$T_o' = F + \beta\left(T_1' + T_2'\right)/2 \tag{19}$$

where

$$F \equiv \left(\alpha T_o + \gamma D\right) + \beta \frac{H'}{2K} \tag{20}$$

It is noticed that the old temperatures and the old heat gain are collected in the parenthesis term of the quantity ”F.”

To calculate heat flux through the wall, the matrix concatenation is carried out. The heat that flows from edge 1 shown in Figure 8 to the center node and the heat that flows from the center node to edge 2 are given by Equation (21).

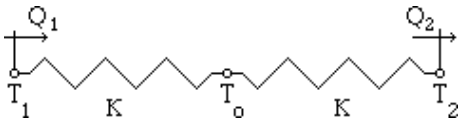

Figure 8 Diagram representing heat flux through the node

$$Q_1 = K(T_1 - T_o) \qquad Q_2 = K(T_o - T_2) \tag{21}$$

Equation (19) for T_o and Equation (20) for the driving temperature is used to express Q_1 and Q_2 successively in matrix form.

$$\begin{pmatrix} Q_1 \\ T_1 \end{pmatrix} = \begin{pmatrix} -K \\ 0 \end{pmatrix} F + \begin{pmatrix} K\left(1 - \frac{\beta}{2}\right) & -K\frac{\beta}{2} \\ 1 & 0 \end{pmatrix} \begin{pmatrix} T_1 \\ T_2 \end{pmatrix} \tag{22}$$

$$\begin{pmatrix} Q_2 \\ T_2 \end{pmatrix} = \begin{pmatrix} K \\ 0 \end{pmatrix} F + \begin{pmatrix} K\frac{\beta}{2} & -K\left(1 - \frac{\beta}{2}\right) \\ 0 & 1 \end{pmatrix} \begin{pmatrix} T_1 \\ T_2 \end{pmatrix} \tag{23}$$

The temperature vector is obtained by solving Equation (22), which is then substituted in Equation (23) to obtain the heat flux and temperature of edge 2 in terms of the respective values of edge 1. The equations in an explicit matrix notation are:

$$\begin{pmatrix} T_1 \\ T_2 \end{pmatrix} = \frac{2}{K\beta} \begin{pmatrix} 0 & K\frac{\beta}{2} \\ -1 & K\left(1 - \frac{\beta}{2}\right) \end{pmatrix} \left\{ \begin{pmatrix} K \\ 0 \end{pmatrix} F + \begin{pmatrix} Q_1 \\ T_1 \end{pmatrix} \right\} \tag{24}$$

$$\begin{pmatrix} Q_2 \\ T_2 \end{pmatrix} = \frac{2}{\beta} \begin{pmatrix} K \\ -1 \end{pmatrix} F + \frac{1}{\beta} \begin{pmatrix} (2-\beta) & -2K(1-\beta) \\ -\frac{2}{K} & (2-\beta) \end{pmatrix} \begin{pmatrix} Q_1 \\ T_1 \end{pmatrix} \tag{25}$$

Results & Analysis

Field Measurement

Based on the empirical data, the energy flux through the envelope is simulated and its average value of 10.86 W/m^2 is found within 7% of the estimated OTTV as described by Equation (1). The annual average rates of energy flux through 8 orientations of the envelope are presented in Table 2. Table 3 and Figure 9 show the monthly average rates of energy flux through 8 orientations of the envelope in each month.

Orientation	**Energy Flux** (W/m^2)
North	3.15
Northeast	10.28
East	15.38
Southeast	13.32
South	7.44
Southwest	13.98
West	15.01
Northwest	8.34
Average	10.86

Table 2 Annual average rates of energy flux through 8 orientations (W/m^2)

(W/m^2)	**Jan.**	**Feb.**	**Mar.**	**Apr.**	**May**	**Jun.**	**Jul.**	**Aug.**	**Sep.**	**Oct.**	**Nov.**	**Dec.**
N	1.79	2.14	2.31	3.93	4.79	5.65	5.05	3.36	2.64	2.29	2.14	1.65
NE	5.61	7.81	10.22	12.71	14.53	15.45	14.89	12.71	10.15	8.08	6.44	4.73
E	13.56	15.23	16.10	17.04	16.19	15.93	16.39	15.98	15.82	15.80	14.07	12.40
SE	17.72	16.15	13.60	10.52	8.88	8.21	8.98	10.52	13.51	15.94	17.97	17.85
S	13.46	9.96	5.68	3.80	3.29	3.26	3.49	3.50	5.85	9.14	13.49	14.33
SW	18.83	17.14	14.59	9.73	9.87	9.05	10.00	9.73	14.54	16.79	18.76	18.77
W	13.26	15.16	15.97	16.44	15.90	15.16	15.72	15.36	15.71	15.49	13.73	12.20
NW	4.22	6.32	8.41	10.33	12.31	12.84	12.33	10.33	8.32	6.32	4.80	3.54
Average	11.06	11.24	10.86	10.56	10.72	10.69	10.86	10.19	10.82	11.23	11.43	10.68

Table 3 Monthly average rates of energy flux through 8 orientations (W/m^2)

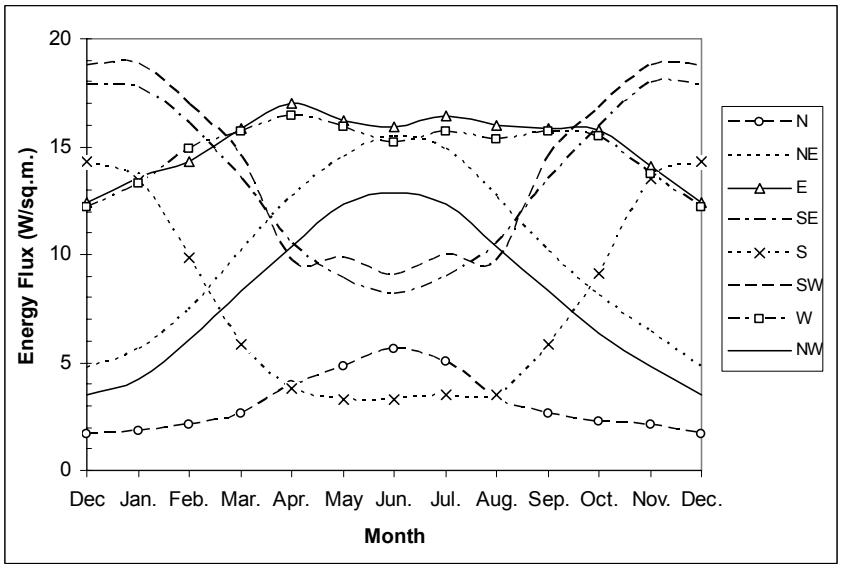

Figure 9 Average rates of energy flux through 8 orientations in each month (W/m^2).

The energy flux by conduction through EIFS walls contributes only 1% to the total energy flux while the combined energy fluxes by conduction (12.5%) and by radiation (86.5%) through heat-stop windows contributes to almost all the total value. Nevertheless, this total value of 10.86 W/m^2 is considered very small because most windows are well protected from the direct radiation.

The outdoor surface temperatures of EIFS walls (26-45C) and heat-stop windows (26-53C), which are greatly affected by solar radiation and diurnal ambient temperatures, have almost no impact on the indoor surface temperature of EIFS walls (28-32C) and slightly affect the indoor surface temperatures of heat-stop windows (28-34C). The outdoor and indoor air temperatures range between 26-37C and 28-32C, respectively.

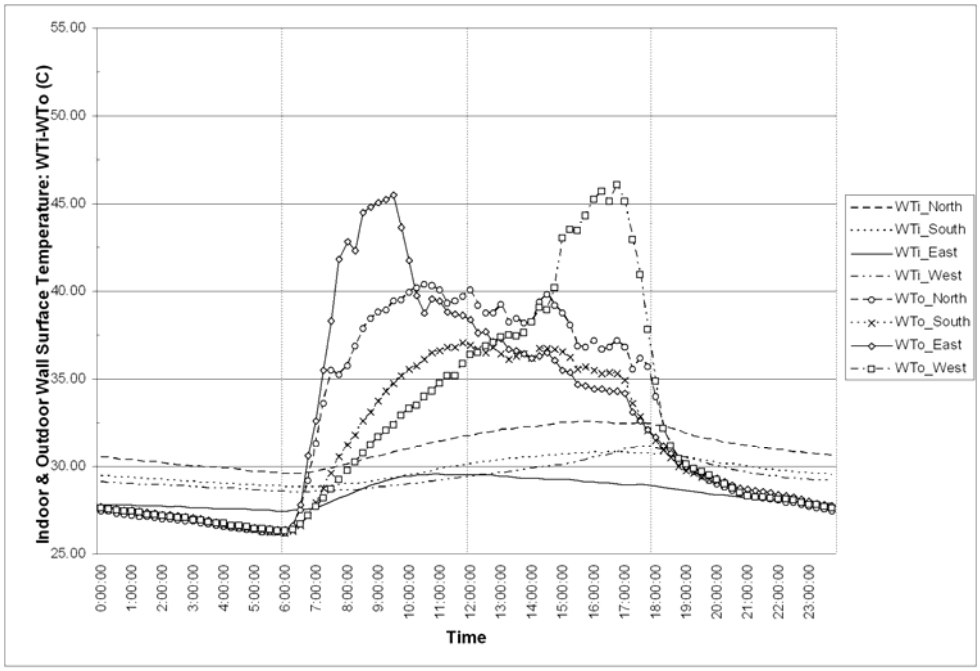

Figure 10 Indoor and outdoor surface temperatures of the EIFS (C).

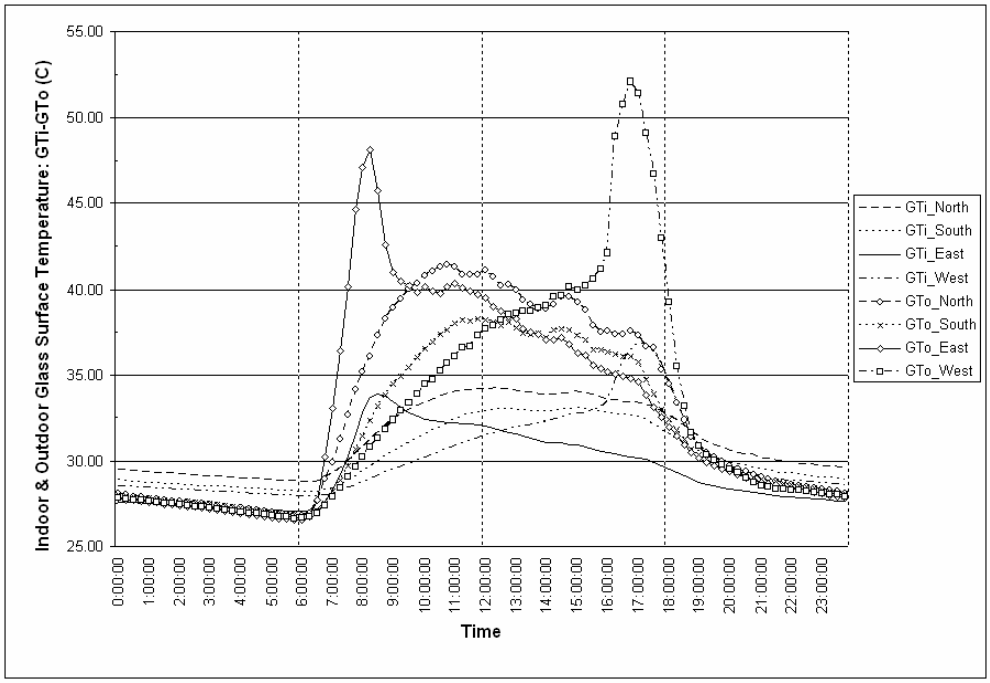

Figure 11 Indoor and outdoor surface temperatures of the heat-stop glass (C).

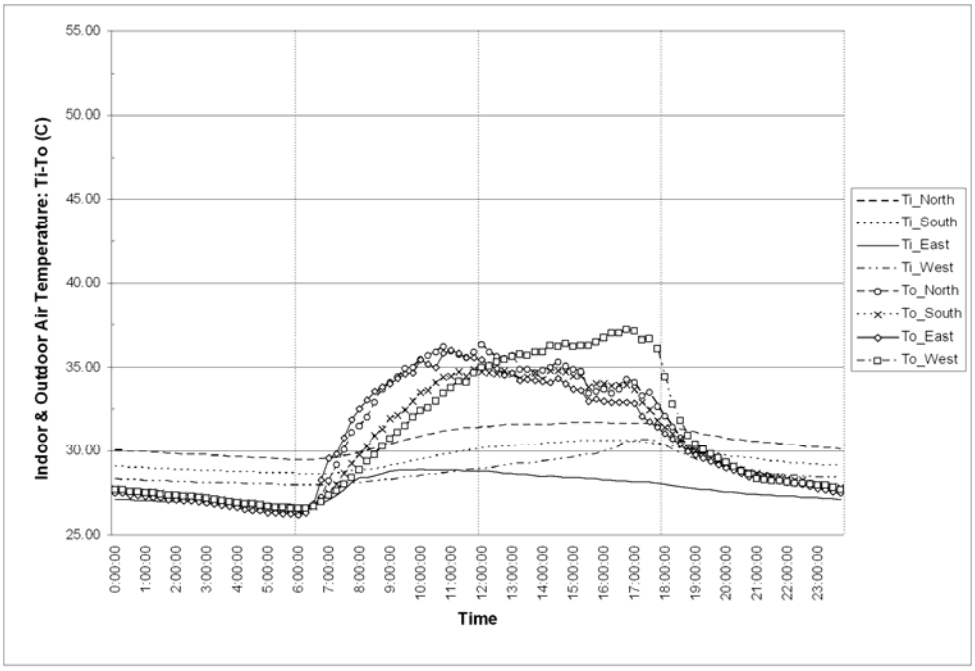

Figure 12 Indoor and outdoor air temperatures (C).

Although the outdoor relative humidity fluctuates extremely (50-95%), the indoor relative humidity remains almost constant (50-60%) throughout the day. The change of the indoor humidity levels is less than 10% of the change of the outdoor humidity levels.

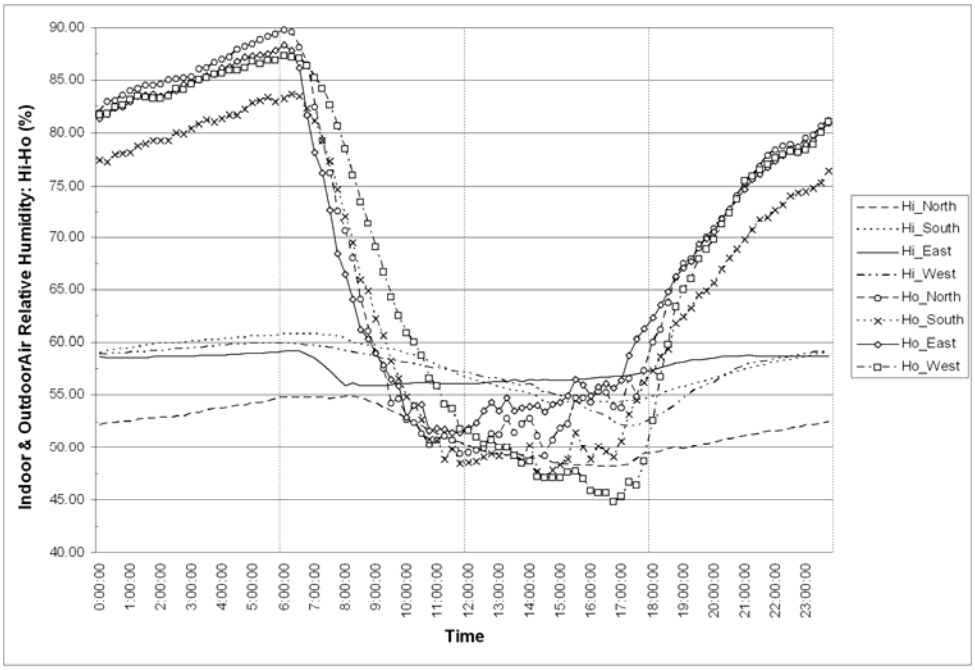

Figure 13 Indoor and outdoor relative humidity (%).

Simulation

The dynamic temperature and heat flux inside both EIFS and other common types of building envelope are simulated using the same outdoor condition from the field measurement. The indoor condition is initialized to the annual average minimum values. Each wall material is subdivided into 7 layers and a node is placed at the center of each layer to monitor the temperature and energy flux inside the wall. Node 1 is placed in the first layer attached to the outdoors while node 7 is placed in the last layer attached to the indoors. Node 4 is located in the middle layer. The dynamic temperature at the node can be calculated using Equations (19) and (20), and based on the node temperatures, the heat flux through the node can be solved by Equation (25). The simulation runs until it reaches the steady-state condition.

Passive Condition

The indoor surface temperatures of the EIFS, 10 cm. brick, and 20 cm. concrete walls in the passive condition are compared. Figure 14 presents hourly average outdoor temperatures (T_o), daily average outdoor temperatures (T_{avg}), and the indoor surface temperatures of different wall materials. During the dynamic steady state condition, the outdoor ambient temperature fluctuates largely between 26C and 35C while the indoor surface temperatures of the EIFS remain almost constant approximately at 29.5C. The indoor surface temperatures of the brick wall range between 27-32C and 28-31C for the concrete wall. Furthermore, the outdoor temperature is peak around 12 pm. while the peak

indoor surface temperatures of the brick and concrete walls occur approximately 4 and 6 hours respectively afterwards. The time lag responses and the peak delays are due to the thermal capacity and thermal mass of the brick and concrete walls.

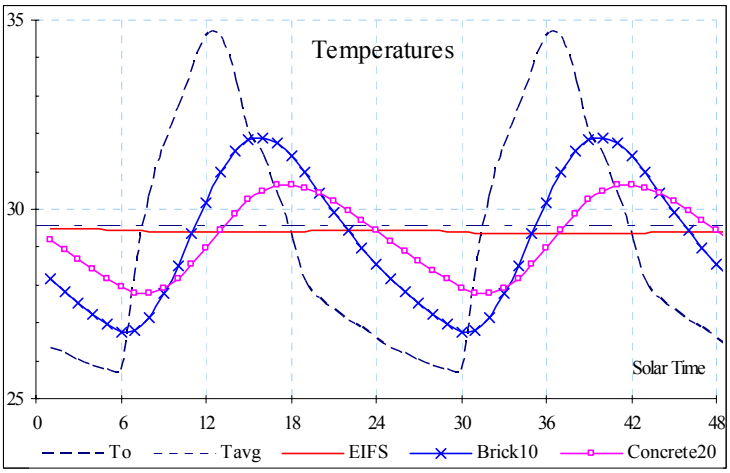

Figure 14 Indoor surface temperatures of EIFS, brick, and concrete walls (C).

The heat flux through the center of each wall (at node 4) is presented in Figure 15. The range of the heat flux (Q_4) for 10 cm. brick and 20 cm. concrete walls are -12-20 W/m^2 and -14-25 W/m^2 respectively while the heat flux for the EIFS is significantly less. Its heat flux range of -0.49 – 0.55 W/m^2 is magnified in Figure 16. It is noted that the negative heat flux during the nighttime means heat flows out of the wall to the outdoors. The negative heat flux of the concrete wall remains around -15 W/m^2 while that of the brick wall gradually decrease from -12 W/m^2 to -5 W/m^2, which indicates that the brick wall losses heat to the outdoors and cools down faster than the concrete wall.

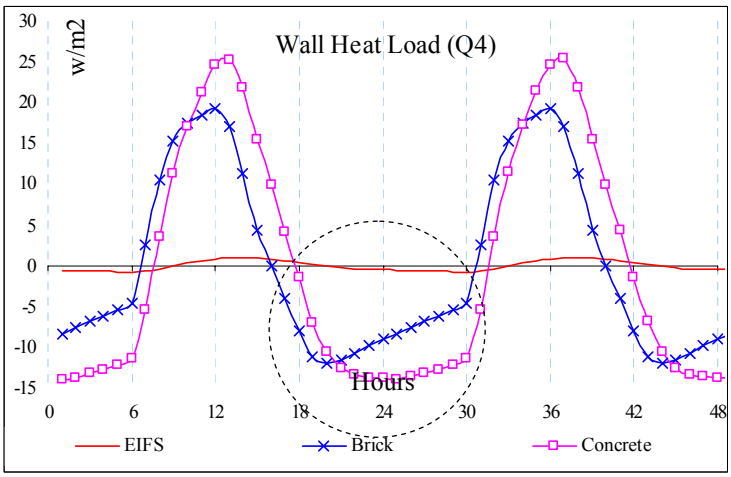

Figure 15 Heat flux through the center of EIFS, brick, and concrete walls (W/m^2).

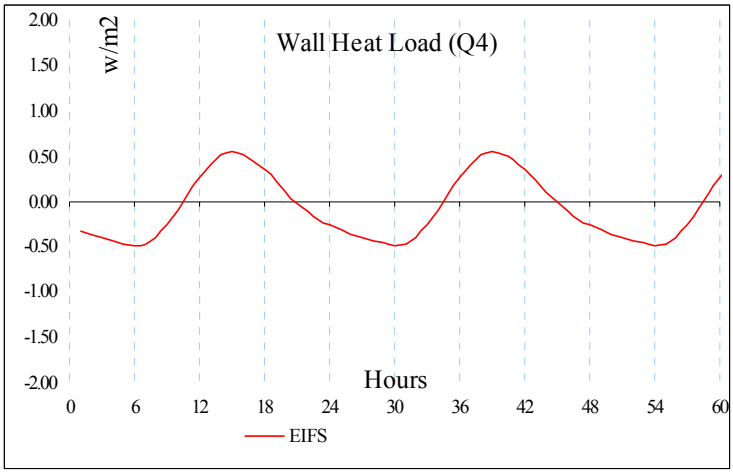

Figure 16 Heat flux through the center of EIFS wall (W/m^2).

The ranges of indoor surface temperatures and heat flux for different wall and window types in the passive environment are summarized in Table 4. The results confirm that the simulated indoor surface temperatures of the EIFS and the heat-stop glass are consistent with those of the field measurement. The agreement of this comparison partially helps validate the simulation results. Consequently, the simulated results of other common envelope types can be considered reliable with some confidences.

Wall & Glass Types	Indoor Surface Temperature (C)	Heat Flux Range (W/m^2)	Average Heat Flux (W/m^2)
EIFS	29.43 – 29.55	-0.61 – 0.85	0.12
Brick 10 cm	26.74 – 31.87	-27.10 – 39.28	6.09
Concrete 20 cm	27.76 – 30.65	-30.17 – 58.43	14.13
Brick with insulation	29.14 – 29.57	-1.93 – 3.07	0.57
Concrete with insulation	29.36 – 29.55	-2.02 – 3.02	0.50
Heat-stop glass	26.13 – 32.96	-10.26 – 13.96	1.85
Double pane glass	25.79 – 34.59	-0.01 – 0.00	0.00

Table 4 Indoor surface temperatures (C) and heat flux (W/m^2) of different envelope types in passive condition

The temperatures and heat flux inside each wall or window type are illustrated by using 3 graphs. The first graph displays the outdoor ambient temperature versus the indoor surface temperature of the wall. The temperatures along the thickness of the wall for 6 different times of the day (4, 8, and 12 in both am & pm) are plotted together in the second graph in order to visualize the diurnal temperature changes inside the wall. This graph can be referred to as, ”Tautochrones Temperatures”. The last graph presents the heat fluxes in 7

different layers along the wall thickness. In Appendix A, Figures A1-A3 show the temperatures and heat flux inside the EIFS, brick, and concrete walls. The simulated results for brick and concrete walls with the 7.5 cm external insulation are presented in Figures A4-A5 as additional samples for composite walls. For the heat-stop and double pane glasses, their results are displayed in Figures A6-A7 respectively.

According to the summary of Table 4, it is noticed that the indoor surface temperatures of the brick and concrete walls with external insulation fluctuate between 29 – 29.6C range, and the heat fluxes are approximately in the range of -2-3 W/m^2. Compared to those of the EIFS, their indoor surface temperatures fall in the same range while the heat fluxes of these walls are slightly higher. The improvement of the brick and concrete walls is solely due to the 7.5 cm external insulation. The tautochrones temperatures of these brick and concrete walls with external insulation (Figures 23 and 24) show that the temperatures decrease proportionally to the thickness of the insulation layer, and reach 29C temperature range at the brick and concrete layers. Furthermore, the indoor surface temperature of the double pane glass is exactly the same as the outdoor surface temperature. The tautochrones temperatures are displayed in all straight lines along the thickness of the glass. Consequently, there is no temperature difference between the outdoor and indoor surface temperatures, and heat flux through the glass is zero. Nevertheless, the heat flux from the hot indoor glass surface to the indoor air is still largely existed.

Active Condition

Figure 17 shows that the indoor surface temperatures of all materials converge to the temperature set point in the simulation, which is 25.5C. The indoor surface temperatures of the EIFS, brick and concrete walls as well as heat-stop and double pane glasses reach 25.5C much faster (18 hours before) than those of the brick and concrete walls with the external insulation.

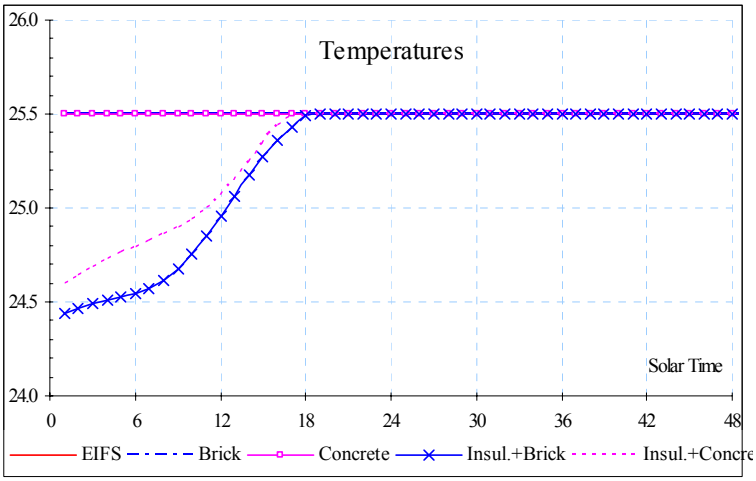

Figure 17 Indoor surface temperatures of EIFS, brick, concrete, brick with insulation, and concrete with insulation walls (C).

The heat fluxes to the indoors (Q7) of different envelope types are displayed in Figure 18. The heat flux range of the concrete wall (5.11 – 21.65 W/m^2) with an average of 13.34 W/m^2, presents the highest value for the opaque walls. The heat flux for the brick wall is also high. Its range and average value are 2.14 – 24.53 W/m^2 and 12.40 W/m^2, respectively. For windows, the heat flux for the double pane glass fluctuates greatly between 1.52 – 48.43 W/m^2 while the heat flux range for heat-stop glass is much lower (0.55 – 13.40 W/m^2) with the average value of 5.88 W/m^2.

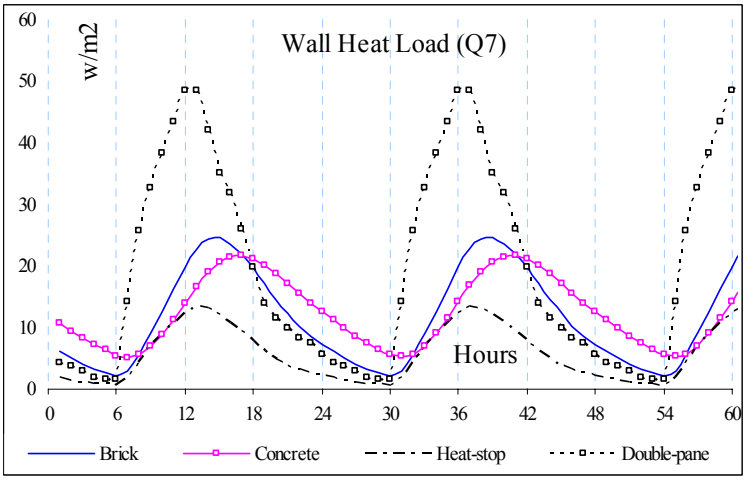

Figure 18 Heat flux to the indoors from the brick and concrete walls, and the heat-stop and double pane windows (W/m^2).

Figure 19 clearly shows that the heat flux of the brick and concrete walls with external insulation reduced significantly. Their heat fluxes ranges -0.058 – 2.75 and -0.057 – 1.52 W/m^2, and the average values are 1.35 and 0.88 W/m^2, respectively. Both heat flux range

(-0.15 – 0.64 W/m^2) and average heat flux value (0.40 W/m^2) of the EIFS are considered small compared to those of other envelope types.

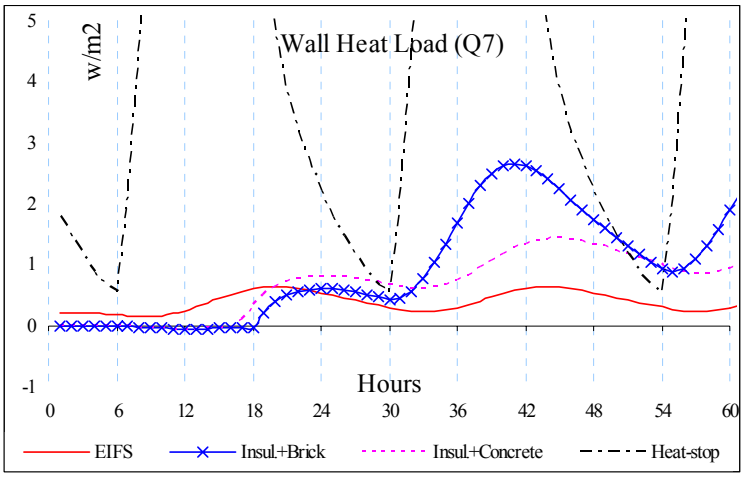

Figure 19 Heat flux to the indoors from the EIFS, concrete, brick with insulation, and concrete with insulation walls (W/m^2).

The results of both indoor surface temperature and heat flux indicate that heat must get through the walls or glasses, and it raises the temperature inside these materials. Once the heat reaches the indoor surface, it becomes the heat load to the indoor space. The time delay and reduced heat load are varied depending on the insulation property and thermal capacity of different materials. For the double pane glass, the heat load to the indoors occurs almost instantaneously while it takes less than an hour for the brick and concrete walls as well as the heat-stop glass. Only small amount of heat gets through the brick and concrete walls with external insulation, and it takes almost 18 hours for the heat load to occur. For the EIFS wall, although the heat load occurs earlier, its magnitude is much less than the heat load to the indoors in other envelope types. It is noticed that the heat load to the indoors occurs at the same time as its indoor surface temperature reaches the thermostat set point.

The heat flux ranges and their average values for different wall and window types in the active environment are summarized in Table 5. Figures A8-A14 in Appendix A display the simulated results of the sample envelope types in the active condition.

Wall & Glass Types	Heat Flux Range (W/m^2)	Average Heat Flux (W/m^2)
EIFS	0.15 – 0.64	0.40
Brick 10 cm	2.14 – 24.53	12.40
Concrete 20 cm	5.11 – 21.65	13.34
Brick with insulation	-0.058 – 2.75	1.35
Concrete with insulation	-0.057 – 1.52	0.88
Heat-stop glass	0.55 – 13.40	5.88
Double pane glass	1.52 – 48.43	19.95

Table 5 Range of heat flux to the indoors and its average (W/m^2) for different envelope types in active condition

Comparisons on Operating and investment Costs

Operating Cost

According to the results from both field measurements and simulations, it is obvious that the Main Hall's envelope outperforms other typical building envelope types. In the active condition, the energy gain by conduction through a 20 cm. concrete wall is 13 times greater than that of the EIFS. By adding 7.5 cm. external insulation, the energy performances of both concrete and brick walls improve significantly. However the energy gains through these walls are still 2-3 times higher than that of the EIFS. Furthermore, the energy gain by conduction through a double pane glass window is approximately 3.5 times greater than that of the heat-stop window, while the energy gain by radiation is about 2 times larger due to the higher Shading Coefficient (SC). The overall energy gain through the double pane windows is more than twice of the heat-stop window. The results are summarized in Table 6.

Wall & Glass Types	Conduction (W/m^2)	Radiation (W/m^2)	Total (W/m^2)
EIFS	0.40	-	0.40
Brick 10 cm	12.40	-	12.40
Concrete 20 cm	13.34	-	13.34
Brick with insulation	1.35	-	1.35
Concrete with insulation	0.88	-	0.88
Heat-stop glass	5.88	9.42	15.30
Double pane glass	19.95	20.72	40.67

Table 6 Average conduction and radiation contributions of energy flux (W/m^2) through different envelope types

From Table 7, the combination of 20 cm concrete walls and double pane windows on the Main Hall's envelope would produce the energy gain of 54.01 W/m^2. By adding 7.5 cm external insulation, the energy gain would be reduced to 41.55 W/m^2. To further improve the energy gain through the envelope, the heat-stop windows may be utilized since the most significant contribution to the energy gain of the Main Hall remains to be the radiation through the windows. Using the 20 cm. concrete wall and the heat-stop windows, the energy gain of 28.64 could be achieved.

Combined Envelope Types	**Energy Flux** (W/m^2)	**Energy Gain** (kBTU/h)	**Cost** (Baht/year)
EIFS & Heat-stop	15.70	99.43	348,405
Brick & Double pane	53.07	413.11	1,447,528
Concrete & Double pane	54.01	425.43	1,490,718
Concrete w/ ins & Double pane	41.55	262.05	918,213
Concrete & Heat-stop	28.64	269.16	943,126

Table 7 Average energy gain (W/m^2) and daily average energy gain (kBTU/h) through different combined envelope types, and estimated operating cost for air conditioning system

In addition, the daily average energy gains through different combined envelope types are also shown Table 7. These results can be used to calculate the operating cost of air conditioning system. Assuming all energy gains through the envelop become the cooling load of the air conditioning system, which has the Seasonal Energy Efficiency Ratio (SEER) equal to 10, and the electricity rate is 4 baht/kWh, the operating cost for air conditioning system to remove this amount of energy gains can be estimated. The use of the EIFS walls and heat-stop windows help save the operating cost for air conditioning system between 0.57-1.14 million baht per year compared to when the brick or concrete wall and the double pane windows are used. The saving would be reduced to less than 0.37 million baht per year if the the 20 cm. concrete wall with external insulation are combined with the heat-stop windows. Thus, the annual operating cost of the air conditioning system due to the energy gains through the actual Main Hall's envelope is approximately 0.57-1.14 million baht less than those of other common envelope types when installed on this building.

Investment cost

The investment costs on the envelope and the air conditioning system are compared. The total investment cost of the Main Hall's envelope is estimated to 17.36 million baht, which 6.53 million baht is invested in the EIFS wall and 10.83 million baht in the heat-stop windows. If the Main Hall was constructed using the concrete walls and double pane windows, 8.70 million baht would be saved on the investment cost. If the external insulation was added on the concrete walls, the saving would be reduced to 6.20 million baht.

Wall & Glass Types	**Unit Price** (Baht/m^2)	**Area** (m^2)	**Total Cost** (million Baht)
EIFS	1,700	3,843	6.53
Brick 10 cm	260	3,843	1.00
Concrete 20 cm	610	3,843	2.34
Brick with insulation	910	3,843	3.50
Concrete with insulation	1,260	3,843	4.84
Heat-stop glass	6,000	1,805	10.83
Double pane glass	3,500	1,805	6.32

Table 8 Unit prices (baht/ m^2) and total investment cost of different envelope types

On the other hand, installing brick or concrete walls and double pane windows on the Main Hall's envelope, the peak cooling demand on the air conditioning system would be 25-50 tons more than the present peak cooling demand. The required capacity of the chillers and other components needs to be increased. This will result in the additional investment cost of 2.92-4.50 million baht for the chillers, pumps and other components of the air conditioning system. In sum, the investment cost of the EIFS wall and the heat-stop windows is approximately 6.20-10.05 million baht more than those of other common envelopes when installed on Main Hall's envelope. However, the installation of EIFS wall and the heat-stop windows reduces the investment cost of the air conditioning system by 2.93-4.50 million baht due to the smaller size of the system. It also reduces the investment cost of the building structure system by 0.51-1.30 million baht since the EIFS wall is 3-8 times lighter than other common envelopes thus the building structure is smaller and costs less. Therefore, only 1.98-5.04 million baht are added to the total investment cost of the Main Hall. Considering the saving of 0.57-1.14 million baht annually on the operating cost of the air conditioning, the simple pay back period with no interest rate would be between 3-

5 years assuming that the lifetime and the maintenance cost of each envelope type are comparable.

	Investment: Envelope (million Baht)	**Additional Investment: Structure** (million Baht)	**Additional Investment: A/C System** (million Baht)	**Operating: A/C System** (million Baht/yr)
EIFS & Heat-stop	17.36	-	-	-
Brick & Double pane	7.32	+ 0.51	+ 4.50	+ 1.10
Concrete & Double pane	8.66	+ 1.30	+ 4.50	+ 1.14
Concrete w/ ins & Double pane	11.16	+ 1.30	+ 2.93	+ 0.57

Table 8 Comparison on investment and operating costs between different combined envelope types

There are some issues relating to the results of this study that should be discussed and may be useful for future researches.

- High humidity level has always been a major problem in a hot humid climate. The Main Hall's envelope has illustrated that it is able to prevent moisture penetration and reduce air infiltration. It significantly decreases the latent heat gain and keeps the indoor humidity at low level. Consequently, the cooling load demand for the air conditioning system is minimized. In this study, however, the effects of the moisture penetration through other common envelope types cannot be completely determined in both field measurements and simulations. Thus, these effects are simplified and partially analyzed in the comparisons of the results.
- The OTTV of the Main Hall is dominated by the contribution from the solar radiation through windows rather than the conduction through walls. On the Main Hall's envelope, the self-shading technique with extended overhangs helps protect its windows from the direct solar radiation while only allow the diffuse radiation to be utilized and therefore reduces the energy gain through the envelope significantly. Furthermore, the circular shape of the Main Hall minimizes the envelope area as well as the surface to floor areas ratio, which in turn decreased the energy gain on the envelope. Due to these reasons, when replacing the envelope of the Main Hall with other common envelope types, the impact on the energy transfer through the envelope will be rather limited, considering the existing geometry of the Main Hall. This impact will be much greater if the same method is applied on other typical buildings with similar floor area.

- Various effective design strategies and construction techniques are implemented to conserve the energy, and economize the construction and the investment costs of the building systems. Smaller sized air conditioning system utilized in the Main Hall would require substantially less maintenance cost, which becomes an additional saving on operating cost of the system. Nevertheless, the maintenance cost is subject for further investigation and is not included in the comparisons.

Conclusion — The results of the analysis both based on the field measurements and the simulations show that the Main Hall's envelope performs well in preventing energy transfer into the building. While its envelope is subjected to a series of diurnal ambient temperature, radiation and humidity cycles, there is relatively no significant effect on the indoor temperature and humidity levels of the Main Hall. The energy flux through the Main Hall's envelope is considerably less than those of other typical envelopes if they were installed on this building. The results of the analysis clearly show that the Main Hall's building envelope outperforms other envelope types in preventing energy transfer into the building.

Although the use of the high energy efficient envelope like the EIFS walls and the heat-stop windows obviously minimizes the operating cost of the air conditioning system, the investment cost of the envelope increases substantially. However, when taking into account the saving on both operating and investment costs of the air conditioning and the structural systems of the building, a simple pay back period of 3-5 years is required for the investment cost of the Main Hall's envelope. Furthermore, it should be noted that greater saving and more favorable pay back period should be obtained if this high energy efficient envelope is applied to other typical buildings, especially those high-rise structures in urban areas. The analysis of additional saving in the air conditioning and other systems is also recommended for further investigation.

Acknowledgement — The Thailand Research Fund (TRF) and Shinawatra University are gratefully acknowledged for funding this research.

References

[1] Praditsmanont, A., Thirakomen, K., Suetrong, N., and Boonyatikarn, S. (2004). Central Academic Building, Shinawatra University: Energy efficient buildings for better quality of life. Unpublished paper reported to ASEAN Energy Awards 2003, July 2004. Award winner for Excellence on Energy Saving Management, ASEAN Energy Awards 2003 held at the 21st ASEAN Ministers of Energy Meeting on June 30-July 4, 2004, Malaysia.

[2] Boonyathikarn, S. (2002). Shinawatra University: An integrated design. Bangkok: GM Max Media, 1st ed.

[3] Bordass, B., Cohen, R., Leaman, A., Ruyssevelt, P., and Standeven, M. (2001). Assessing building performance in use (Parts 1-5). Building Research and Information, 29(2), 85–157.

[4] Chungloo, S., Limmeechokchai, B., and Chungpaibulpatana, S. (2001). Parametric analysis of energy efficient building envelopes in Thailand, Asian Journal of Energy & Environment, 2(2), 137-155.

[5] Chaiyapinunt, S. (2005). Standard Meteorological Data for using with Energy Simulation Computer Program for building. Unpublished report sponsored by TRF, December 2005.

[6] Chaiyapinunt, S. and Mangkornsaksit, K. (2002). The Use of Meteorological Data in TRY Format in a DOE-2.1E Simulation, Journal of Energy, Heat and Mass Transfer, Vol.24, 163-173.

[7] Chaiyapinunt, S. and Mangkornsaksit, K. (2001). Standard Meteorological Data for Bangkok, Journal of Energy, Heat and Mass Transfer, Vol.23, 33-37

[8] Chaiyapinunt, S. and Mankornsaksit, K. (2000). Mathematical Models for Hourly Diffuse Solar Radiation at Bangkok, Journal of Energy, Heat and Mass Transfer, 1-6.

[9] American Society of Heating Refrigerating and Air Conditioning Engineers (1980). Energy conservation in new building design, ASHRAE Standard 90A-1980. Atlanta, GA: ASHRAE.

[10] American Society of Heating Refrigerating and Air Conditioning Engineers (1993). ASHRAE handbook 1985 fundamentals. Atlanta, GA: ASHRAE.

[11] Chairarattananon, S., Rakwamsuk, P., Hien, V. D., and Taweekun, J. (2004). Development of a Building Energy Code for New Buildings in Thailand, Proceedings of the Joint International Conference on ”Sustainable Energy and Environment (SEE)”, December 1-3, 2004, Hua Hin, Thailand.

[12] Arumí-Noé, F. N. & Burch, D. M. (1984). DEROB Simulation of the NBS Thermal Mass Test Buildings. ASHRAE Transactions, 2B, Atlanta, Ga.

[13] Arumí-Noé, F. N. (1980). Continued development and physical validation of computer program DEROB. Proceedings of US Department of Energy Passive & Hybrid Solar Energy Program update meeting, Sept 21-24, 1980 Washington, DC, 69-72.

[14] Arumí-Noé, F. N. (1985). Theory reports and validation studies on the computer code DEROB. Unpublished paper reported to the Solar Heating and Cooling Research and Development Branch, Office of Conservation and Solar Application, U.S. Department of Energy.

Appendices

Appendix A: Temperatures and Heat Flux inside Different Envelope Types in Passive and Active Conditions

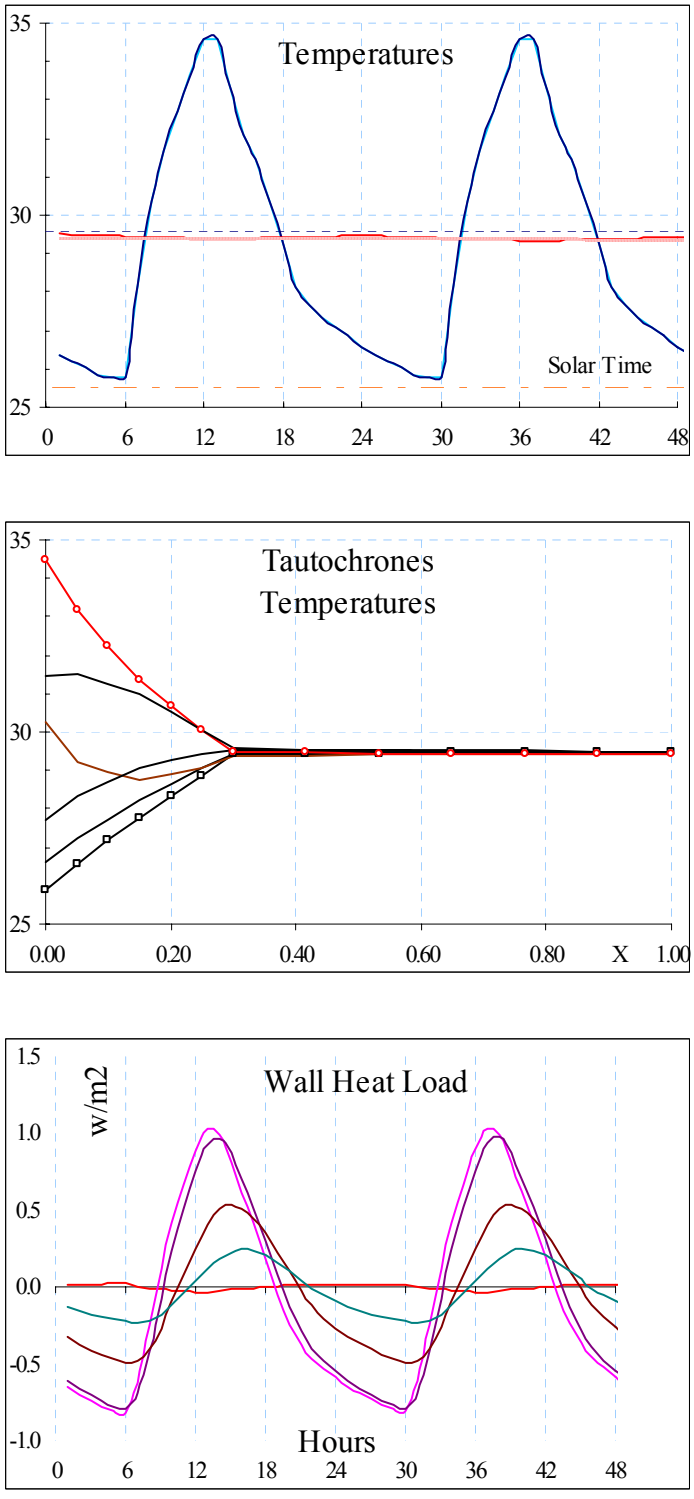

Figure A1 Temperatures and heat flux inside the EIFS wall in passive condition.

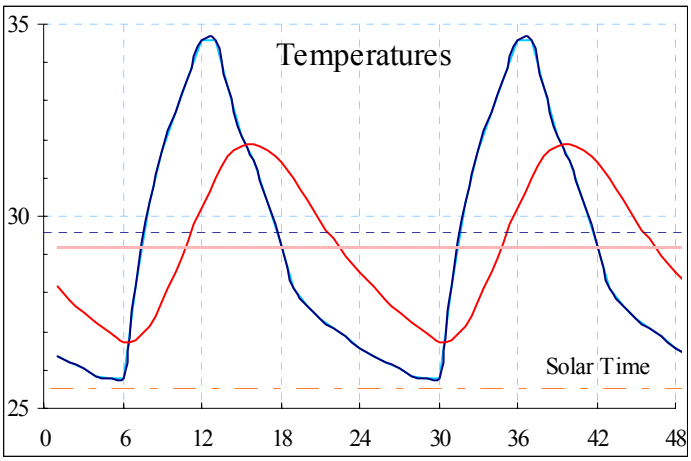

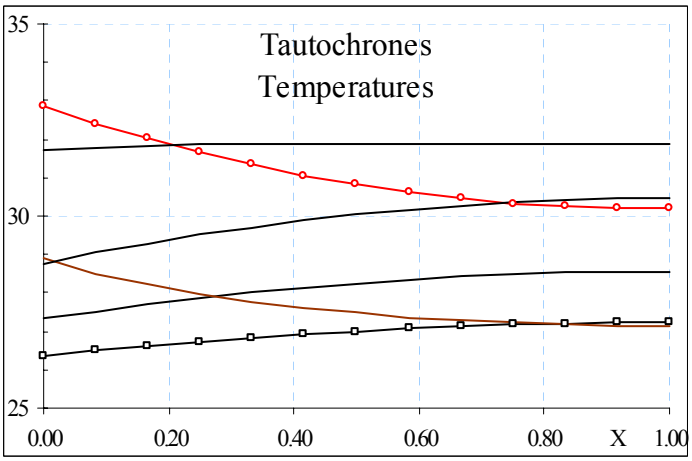

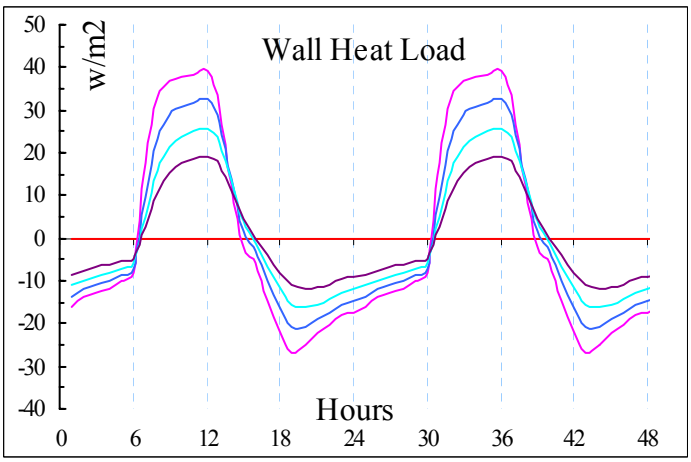

Figure A2 Temperatures and heat flux inside the 10 cm brick wall in passive condition.

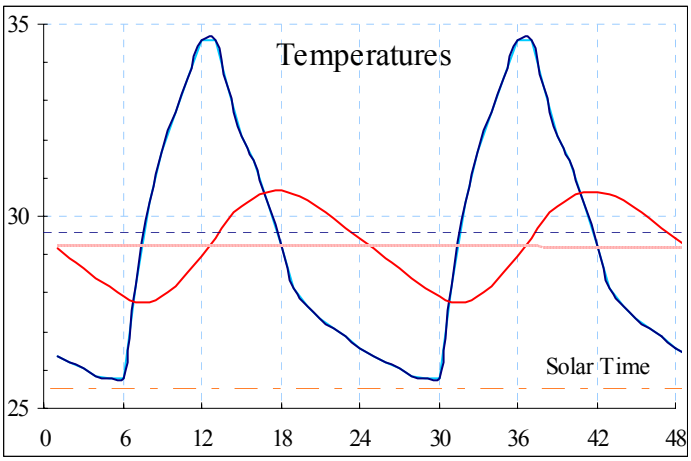

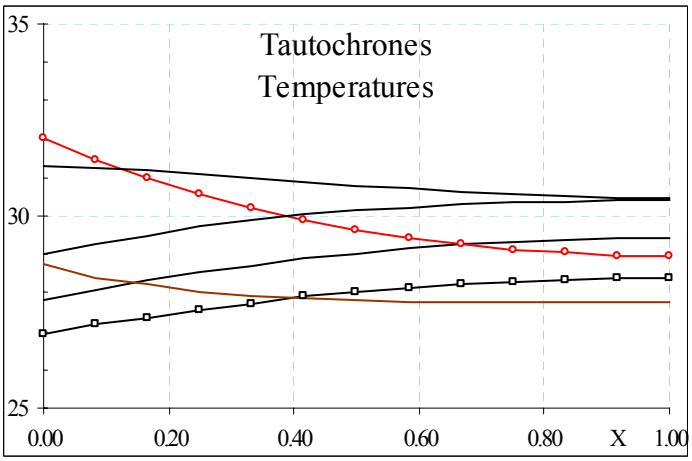

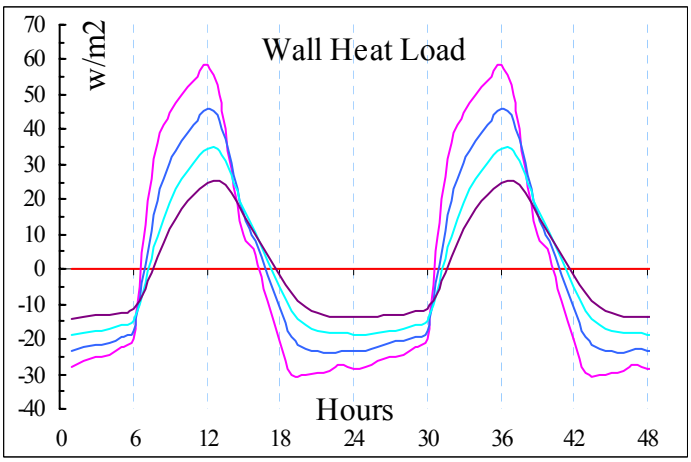

Figure A3 Temperatures and heat flux inside the 20 cm concrete wall in passive condition.

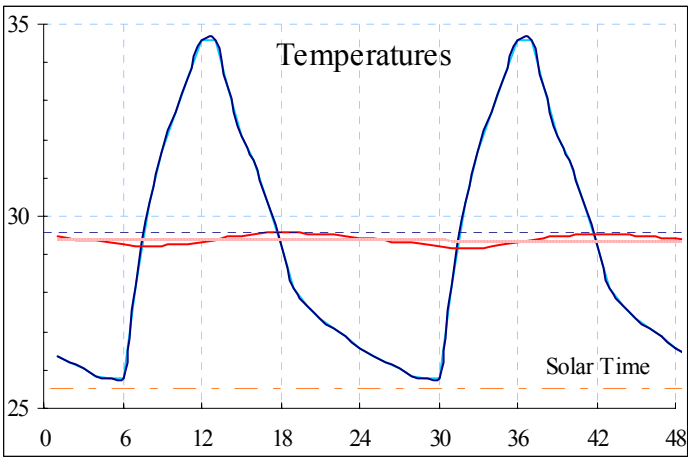

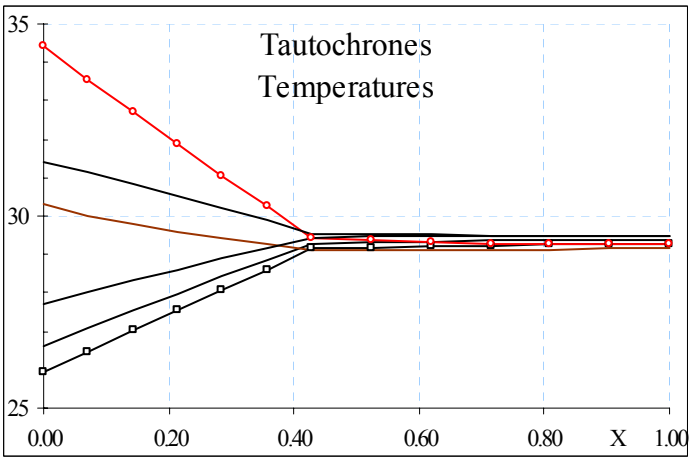

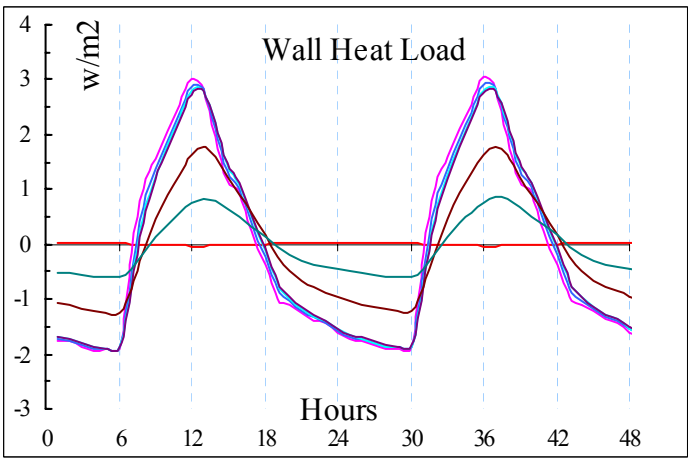

Figure A4 Temperatures and heat flux inside the 10 cm brick wall with 7.5 cm external wool insulation in passive condition.

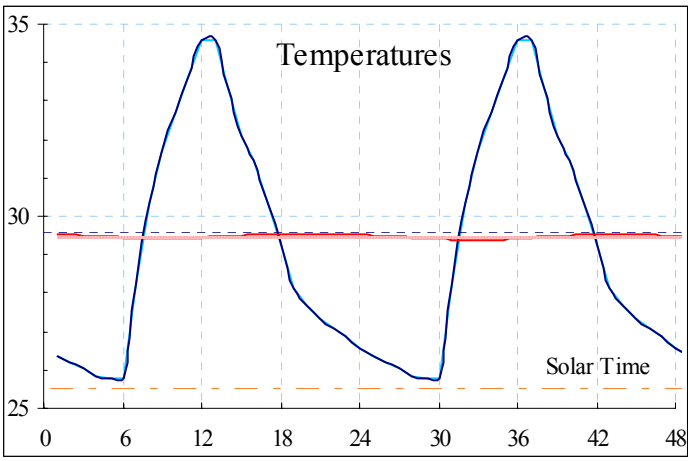

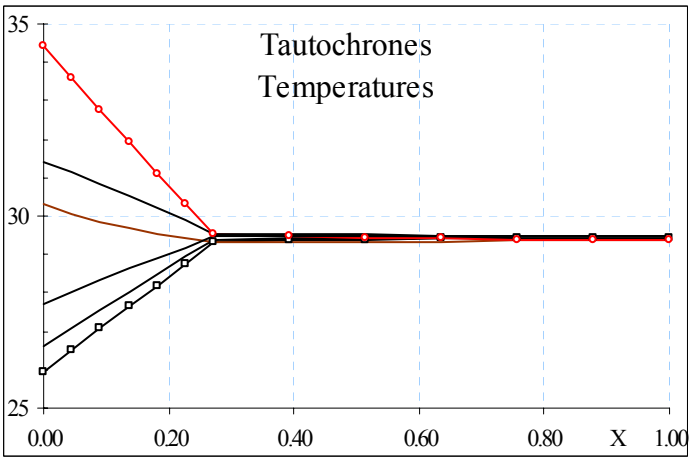

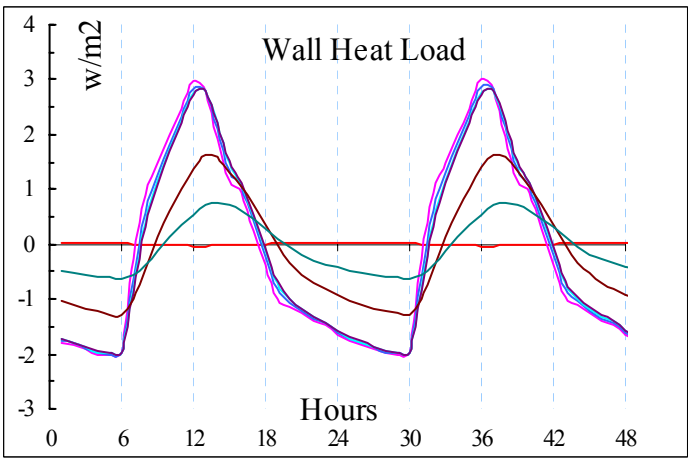

Figure A5 Temperatures and heat flux inside the 20 cm concrete wall with 7.5 cm external wool insulation in passive condition.

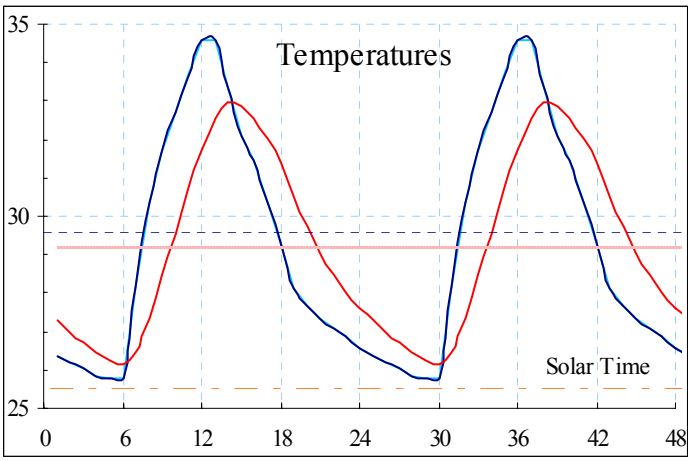

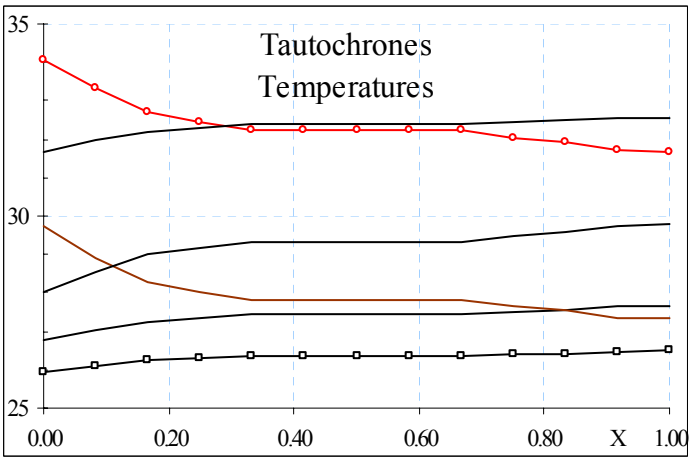

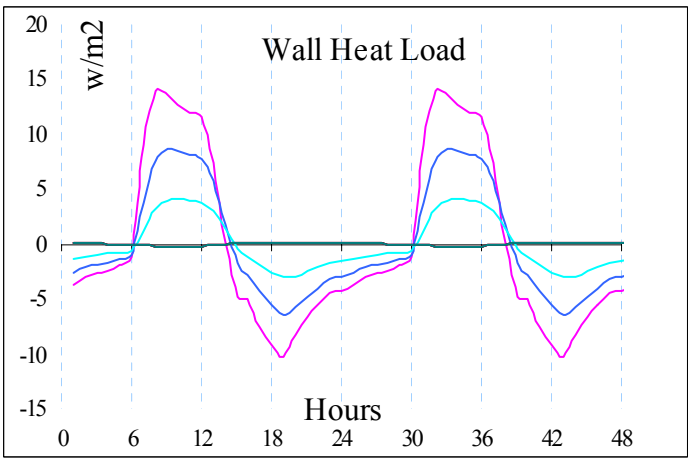

Figure A6 Temperatures and heat flux inside the heat-stop glass in passive condition.

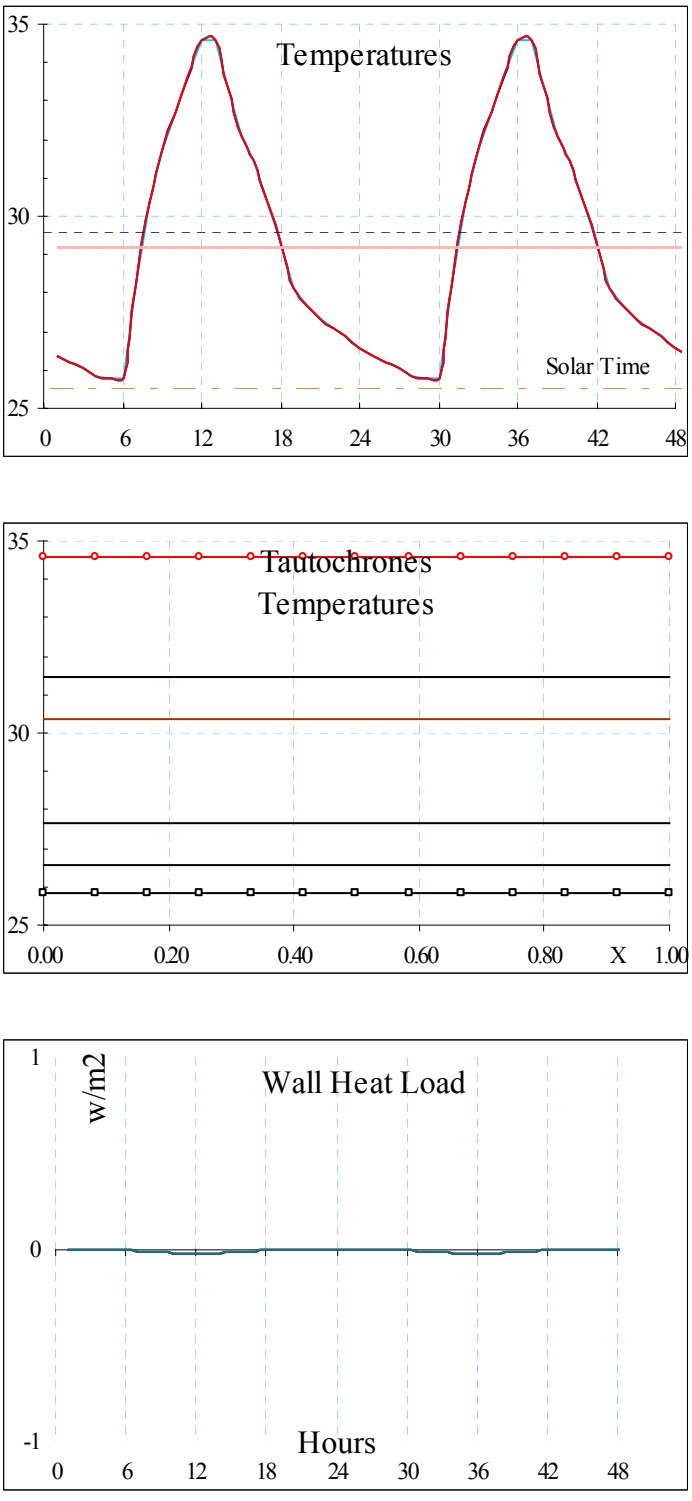

Figure A7 Temperatures and heat flux inside the double pane glass in passive condition.

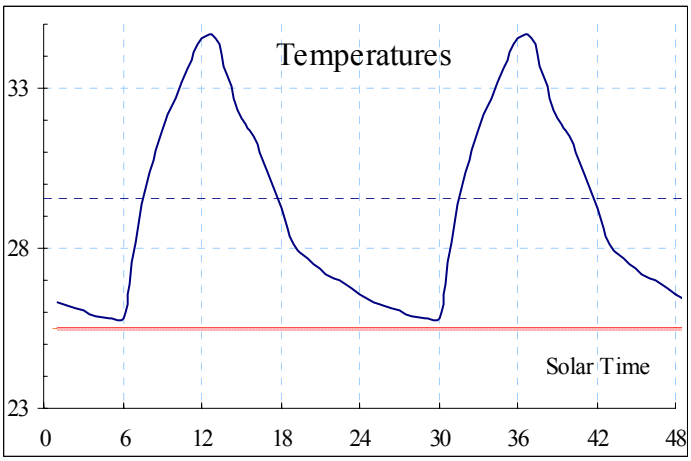

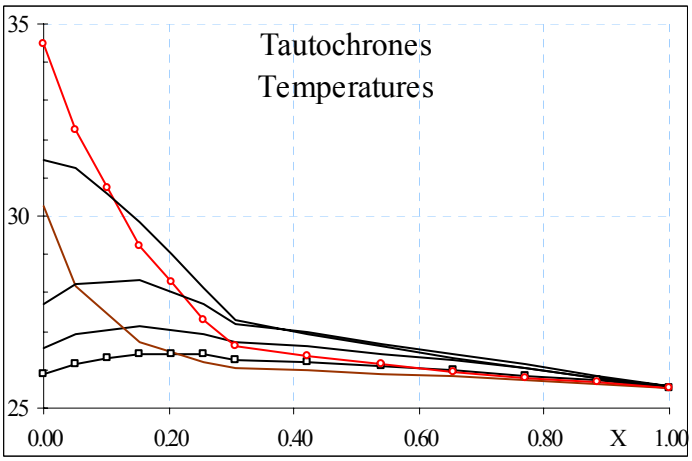

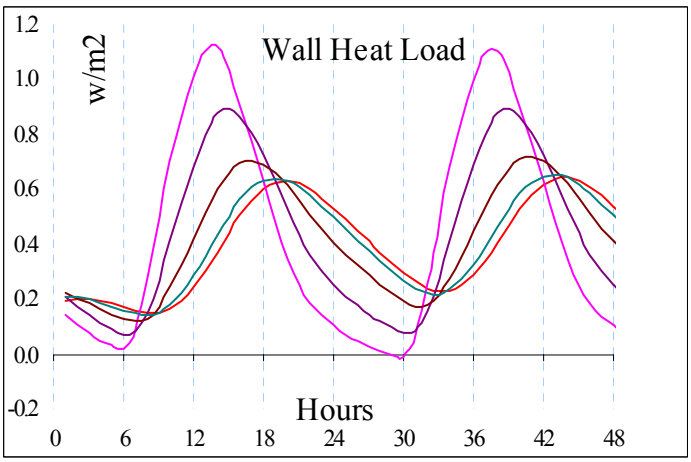

Figure A8 Temperatures and heat flux inside the EIFS wall in active condition.

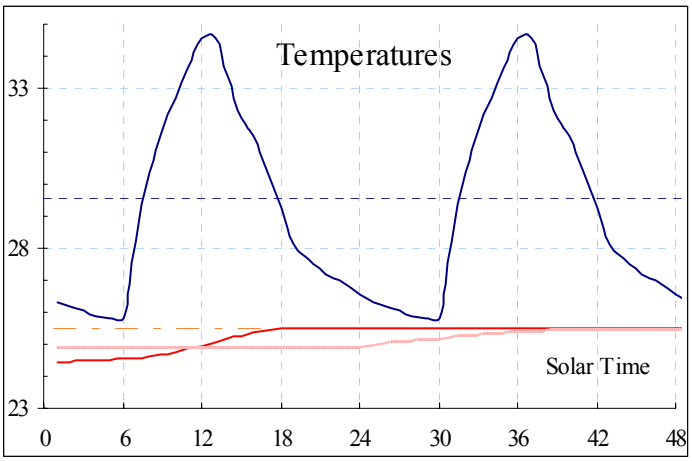

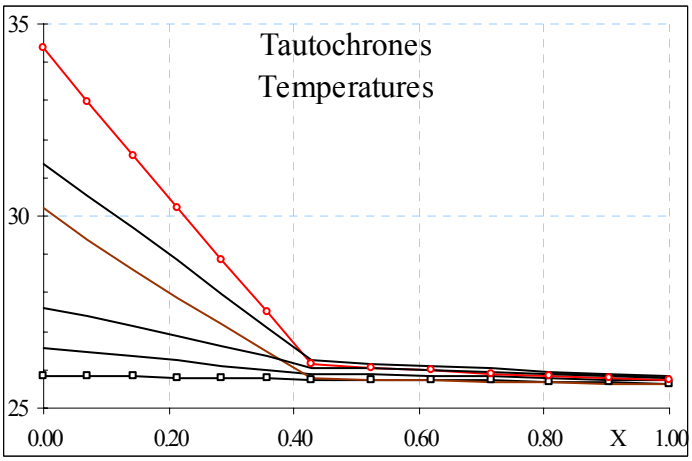

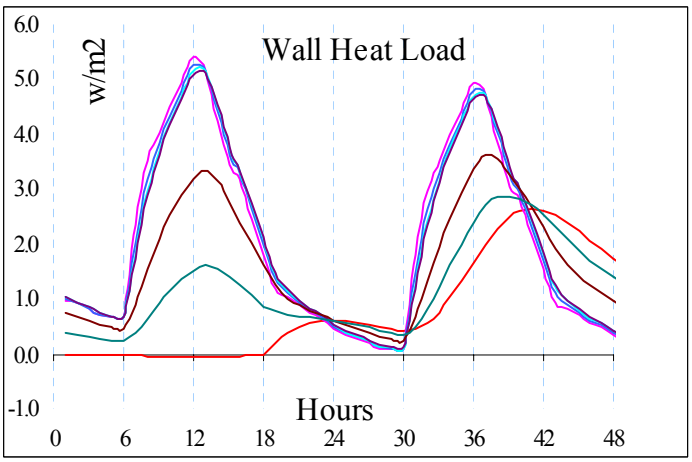

Figure A9 Temperatures and heat flux inside the 10 cm brick wall with 7.5 cm external wool insulation in active condition.

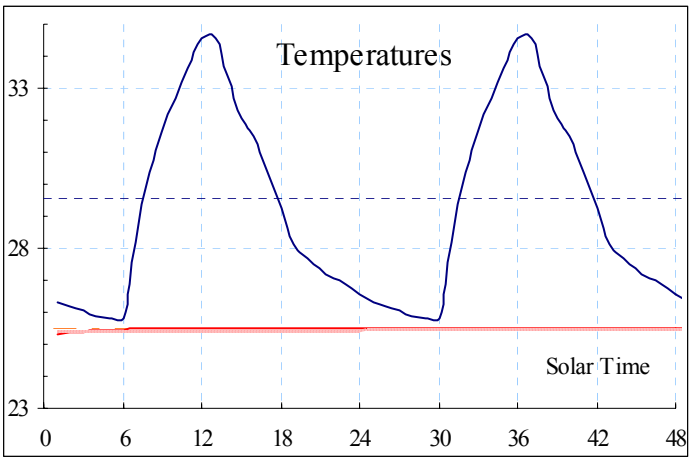

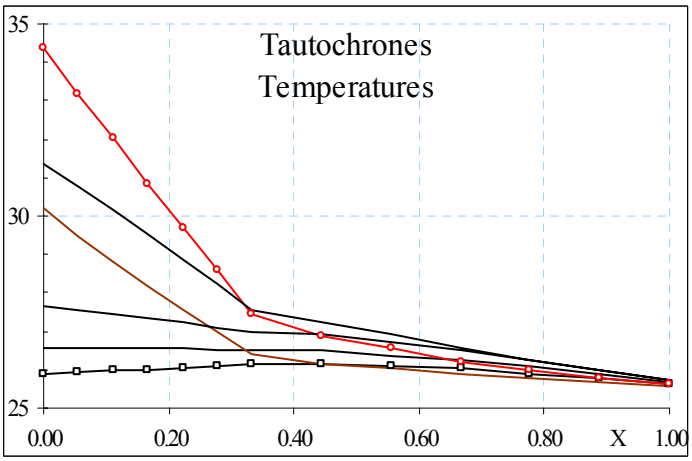

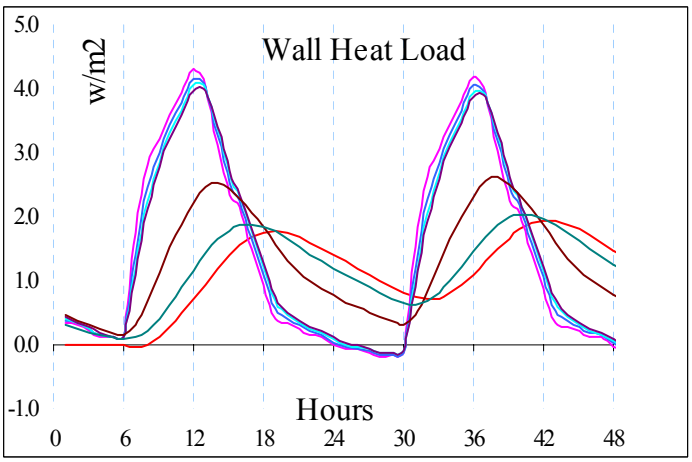

Figure A10 Temperatures and heat flux inside the 20 cm concrete wall with 7.5 cm external wool insulation in active condition.

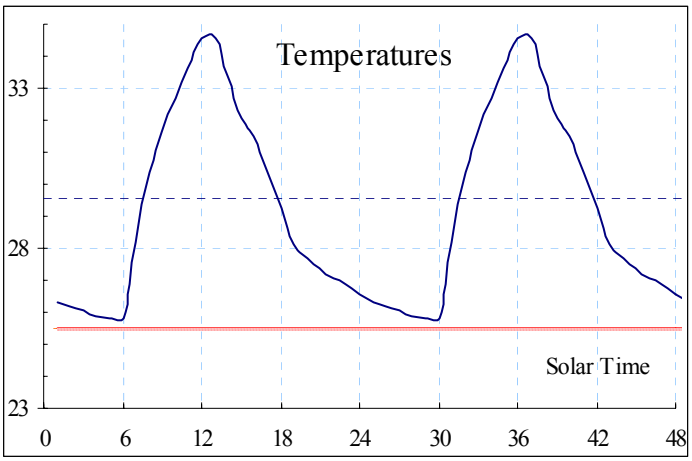

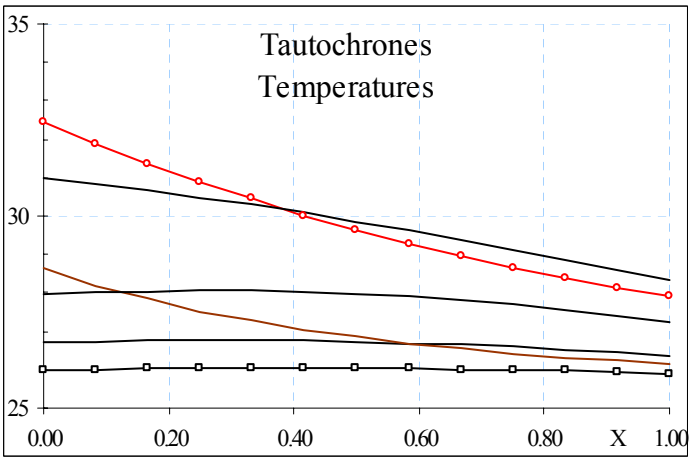

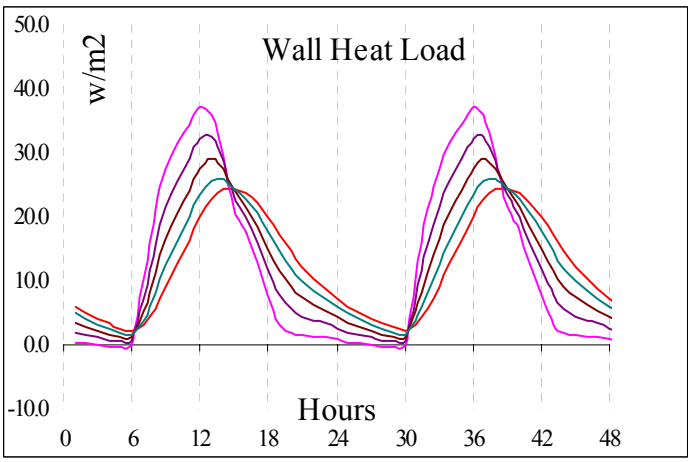

Figure A11 Temperatures and heat flux inside the 10 cm brick wall in active condition.

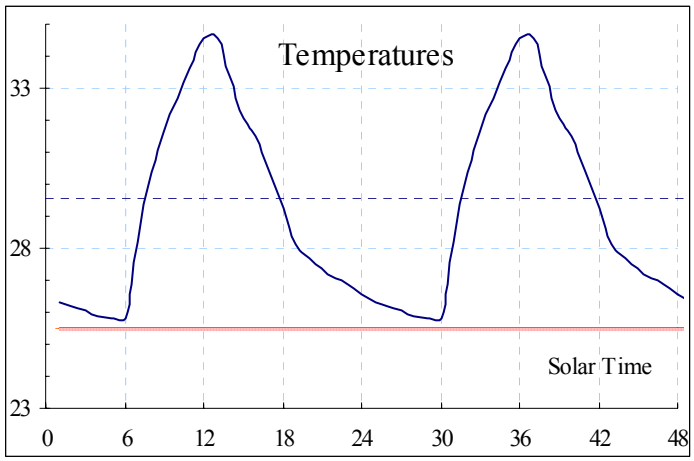

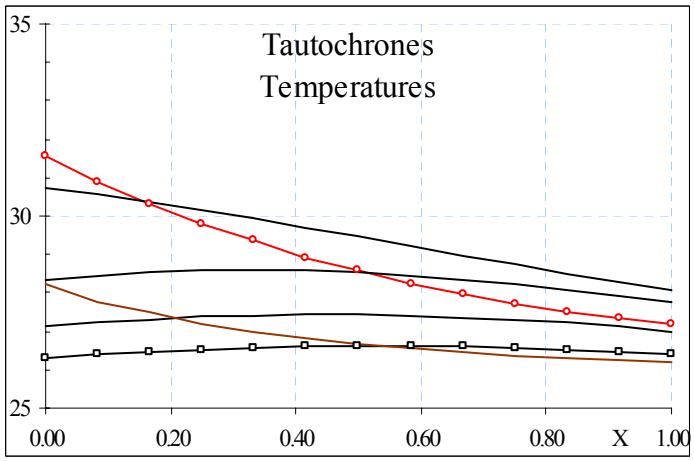

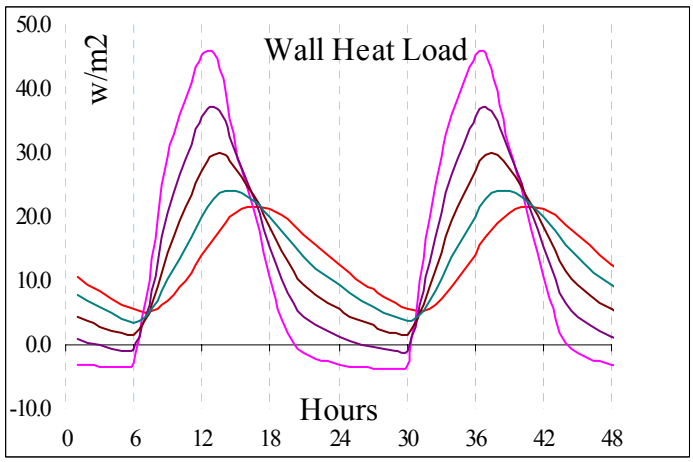

Figure A12 Temperatures and heat flux inside the 20 cm concrete wall in active condition.

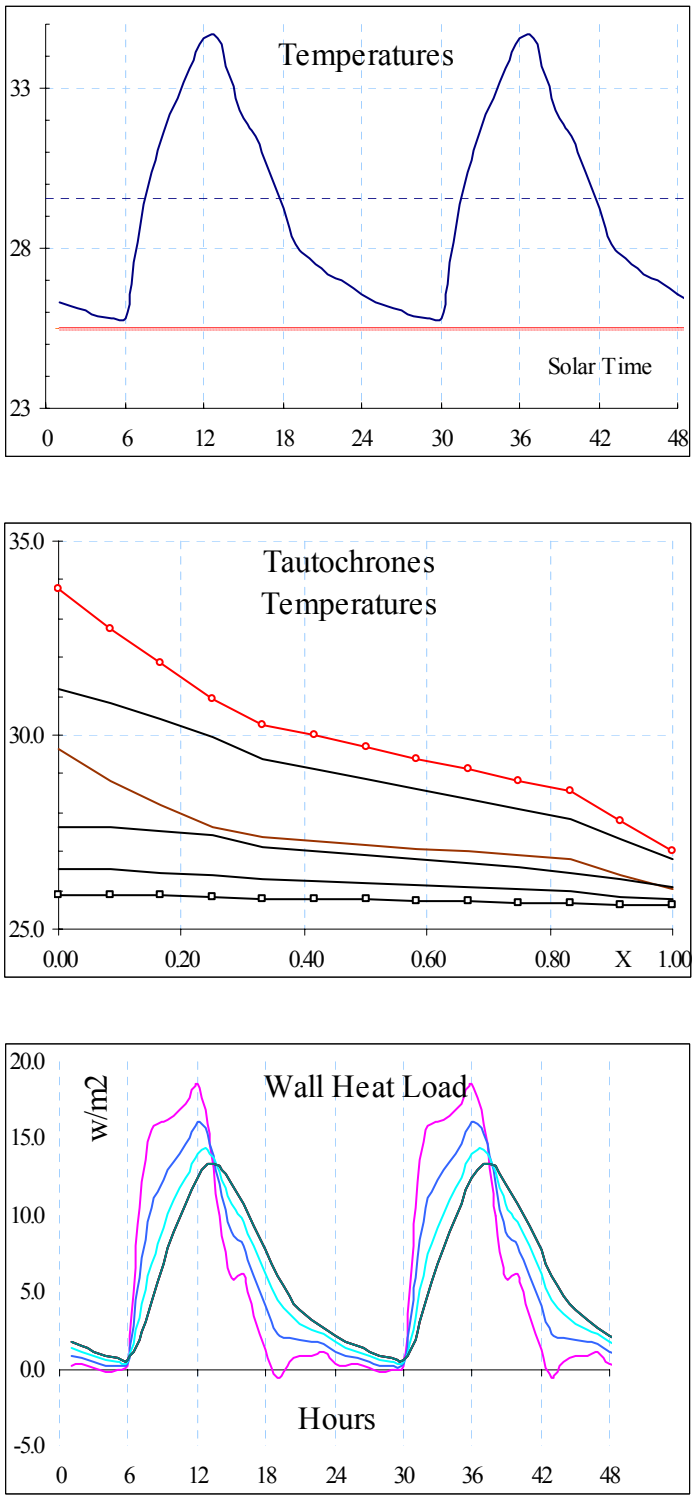

Figure A13 Temperatures and heat flux inside the heat-stop glass in active condition.

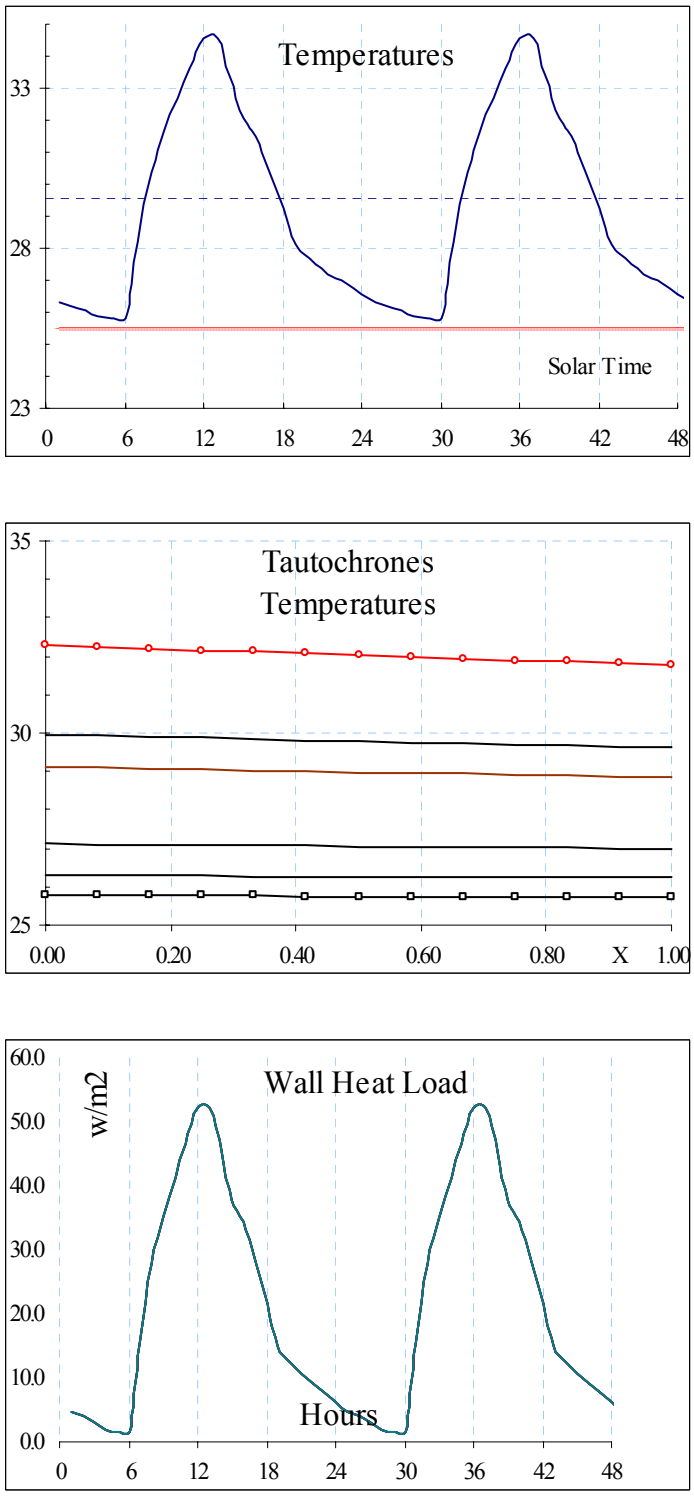

Figure A14 Temperatures and heat flux inside the double pane glass in active condition.

Appendix B: Example of Meteorological Data: Pathumthani Province, January 1-2, 1995

Year	Month	Date	Time	DRY	WET	RH	RAIN	CLD	RADI	DIR	SPD
1995	1	1	1	22.9	20.8	82	0	5	-	0	0
1995	1	1	2	22.4	20.5	83	0	4	-	0	0
1995	1	1	3	22	20.4	88	0	4	-	0	0
1995	1	1	4	21.5	20.1	87	0	4	-	0	0
1995	1	1	5	21	19.7	88	0	4	0.04	0	0
1995	1	1	6	21	20	91	0	4	0.06	0	0
1995	1	1	7	21.2	20.2	91	0	6	0.35	0	0
1995	1	1	8	23	21.3	85	0	5	1.01	0	0
1995	1	1	9	26	21.7	68	0	4	1.8	0	0
1995	1	1	10	27.4	22.1	61	0	4	2.4	0	0
1995	1	1	11	30	22.9	50	0	4	2.66	0	0
1995	1	1	12	31	22.9	45	0	6	2.78	10	5
1995	1	1	13	31	22.4	42	0	5	2.85	20	4
1995	1	1	14	31.6	22.8	41	0	5	2.44	50	4
1995	1	1	15	31.5	22.2	39	0	5	1.82	90	4
1995	1	1	16	31.4	22.5	41	0	5	0.99	10	3
1995	1	1	17	31	22.3	41	0	4	0.25	0	0
1995	1	1	18	29.3	23.1	57	0	6	0.03	0	0
1995	1	1	19	28	22.3	59	0	5	0.02	0	0
1995	1	1	20	26	21.9	68	0	4	-	0	0
1995	1	1	21	26	22.1	70	0	4	-	0	0
1995	1	1	22	25.9	23.2	79	0	4	-	0	0
1995	1	1	23	25	22.9	83	0	4	-	0	0
1995	1	1	24	24	22	83	0	4	-	0	0
1995	1	2	1	23.2	21.8	88	0	4	-	0	0
1995	1	2	2	22.8	21.5	89	0	4	-	0	0
1995	1	2	3	22.4	21.2	89	0	4	-	0	0
1995	1	2	4	22	21	91	0	4	-	0	0
1995	1	2	5	21.8	21	93	0	4	0.04	0	0
1995	1	2	6	21.7	21	94	0	4	0.07	0	0
1995	1	2	7	22	21.2	93	0	4	0.38	0	0
1995	1	2	8	22.9	21.8	90	0	4	1	0	0
1995	1	2	9	25.7	22.8	77	0	4	1.75	0	0
1995	1	2	10	28	23.2	65	0	4	2.36	0	0
1995	1	2	11	29	23.5	61	0	4	2.64	0	0
1995	1	2	12	30	23	50	0	6	2.86	30	4
1995	1	2	13	30.9	23.2	47	0	7	2.83	80	7
1995	1	2	14	31.3	23.2	45	0	7	2.25	60	5
1995	1	2	15	32	24.1	47	0	7	1.22	30	4
1995	1	2	16	31.9	24.8	52	0	7	0.83	0	0
1995	1	2	17	31.1	24.6	54	0	7	0.23	0	0
1995	1	2	18	30	23.8	55	0	7	0.04	0	0
1995	1	2	19	28.2	23	62	0	7	0.04	0	0
1995	1	2	20	27	23	70	0	6	-	0	0
1995	1	2	21	25.8	22.2	72	0	5	-	0	0
1995	1	2	22	25	22	76	0	5	-	0	0
1995	1	2	23	24.2	22	82	0	5	-	0	0
1995	1	2	24	24.1	22	82	0	4	-	0	0

Appendix C: Example of Solar Table - Latitude 14 North

Solar Table: Latitude 14 North

	Hour	Alt	Azi	South	North	East/W	Zenith	Sky	Ground	Beam
Dec	6:27	0.00	65.62	0.41	0.00	0.91	0.00	0.00	0.00	0.00
	7: 0	7.24	63.24	0.45	0.00	0.89	0.13	0.25	0.28	0.23
	8: 0	19.82	57.58	0.50	0.00	0.79	0.34	0.31	0.47	0.48
	9: 0	31.53	49.54	0.55	0.00	0.65	0.52	0.27	0.57	0.57
	10: 0	41.53	37.77	0.59	0.00	0.46	0.66	0.23	0.64	0.62
	11: 0	48.76	21.11	0.61	0.00	0.24	0.75	0.20	0.69	0.65
	12: 0	51.44	0.00	0.62	0.00	0.00	0.78	0.19	0.70	0.66
	Daily Totals (hrs/day)			3.22	0.00	1.35	3.28	2.59	5.87	
Jan/Nov	6:23	0.00	68.90	0.36	0.00	0.93	0.00	0.00	0.00	0.00
	7: 0	8.28	66.23	0.40	0.00	0.91	0.14	0.26	0.30	0.26
	8: 0	21.22	60.58	0.46	0.00	0.81	0.36	0.30	0.48	0.49
	9: 0	33.37	52.54	0.51	0.00	0.66	0.55	0.27	0.59	0.59
	10: 0	43.95	40.63	0.55	0.00	0.47	0.69	0.22	0.66	0.63
	11: 0	51.63	23.01	0.57	0.00	0.24	0.78	0.19	0.70	0.66
	12: 0	54.59	0.00	0.58	0.00	0.00	0.81	0.17	0.72	0.66
	Daily Totals (hrs/day)			3.04	0.00	1.44	3.51	2.55	6.06	
Feb/Oct	6:13	0.00	77.83	0.21	0.00	0.98	0.00	0.00	0.00	0.00
	7: 0	11.07	74.50	0.26	0.00	0.95	0.19	0.29	0.35	0.34
	8: 0	24.83	69.11	0.32	0.00	0.85	0.42	0.30	0.52	0.53
	9: 0	37.95	61.40	0.38	0.00	0.69	0.61	0.25	0.62	0.61
	10: 0	50.00	49.60	0.42	0.00	0.49	0.77	0.19	0.69	0.65
	11: 0	59.32	29.77	0.44	0.00	0.25	0.86	0.16	0.74	0.67
	12: 0	63.13	0.00	0.45	0.00	0.00	0.89	0.14	0.75	0.68
	Daily Totals (hrs/day)			2.40	0.00	1.64	4.07	2.44	6.51	
Mar/Sep	6: 0	0.00	90.00	0.00	0.00	1.00	0.00	0.00	0.00	0.00
	7: 0	14.42	85.82	0.07	0.00	0.97	0.25	0.30	0.40	0.40
	8: 0	28.82	81.27	0.13	0.00	0.87	0.48	0.28	0.55	0.56
	9: 0	43.08	75.49	0.18	0.00	0.71	0.68	0.22	0.65	0.63
	10: 0	56.72	65.67	0.22	0.00	0.50	0.84	0.17	0.73	0.67
	11: 0	68.91	45.99	0.25	0.00	0.26	0.93	0.13	0.77	0.69
	12: 0	74.80	0.00	0.26	0.00	0.00	0.96	0.11	0.78	0.69
	Daily Totals (hrs/day)			1.25	0.00	1.83	4.67	2.32	6.99	
Apr/Aug	5:47	0.00	102.17	0.00	0.21	0.98	0.00	0.00	0.00	0.00
	6: 0	2.98	101.37	0.00	0.20	0.98	0.05	0.14	0.14	0.07
	7: 0	17.28	97.96	0.00	0.13	0.95	0.30	0.31	0.44	0.44
	8: 0	31.67	94.99	0.00	0.07	0.85	0.53	0.27	0.58	0.58
	9: 0	46.14	92.47	0.00	0.02	0.69	0.72	0.21	0.67	0.64
	9:24	51.81	86.91	0.00	0.00	0.62	0.79	0.19	0.70	0.66
	10: 0	60.58	85.15	0.02	0.00	0.49	0.87	0.15	0.74	0.68
	11: 0	75.02	78.55	0.05	0.00	0.25	0.97	0.11	0.78	0.69
	12: 0	86.38	0.00	0.06	0.00	0.00	1.00	0.10	0.80	0.70
	Daily Totals (hrs/day)			0.13	0.23	1.90	5.02	2.38	7.40	
May/Jul	5:37	0.00	111.11	0.00	0.36	0.93	0.00	0.00	0.00	0.00
	6: 0	5.16	109.71	0.00	0.34	0.94	0.09	0.21	0.22	0.16
	6: 0	5.16	109.71	0.00	0.34	0.94	0.09	0.21	0.22	0.16
	7: 0	18.91	106.81	0.00	0.27	0.91	0.32	0.31	0.46	0.46
	8: 0	32.82	104.94	0.00	0.21	0.81	0.54	0.27	0.58	0.58
	9: 0	46.89	104.06	0.00	0.16	0.66	0.73	0.21	0.68	0.64
	10: 0	60.93	105.26	0.00	0.12	0.47	0.87	0.15	0.74	0.68
	11: 0	74.58	114.13	0.00	0.10	0.24	0.96	0.12	0.78	0.69
	12: 0	84.27	180.00	0.00	0.09	0.00	0.99	0.10	0.80	0.70
	Daily Totals (hrs/day)			0.00	1.16	1.91	5.11	2.49	7.59	
Jun	5:33	0.00	114.39	0.00	0.41	0.91	0.00	0.00	0.00	0.00
	6: 0	5.91	112.79	0.00	0.39	0.92	0.10	0.22	0.24	0.19
	6: 0	5.91	112.79	0.00	0.39	0.92	0.10	0.22	0.24	0.19
	7: 0	19.39	110.10	0.00	0.32	0.89	0.33	0.31	0.46	0.47
	8: 0	33.09	108.56	0.00	0.27	0.79	0.55	0.27	0.59	0.58
	9: 0	46.80	108.68	0.00	0.22	0.65	0.73	0.21	0.68	0.64
	10: 0	60.46	111.57	0.00	0.18	0.46	0.87	0.15	0.74	0.68
	11: 0	73.34	124.14	0.00	0.15	0.24	0.96	0.12	0.78	0.69
	12: 0	81.49	180.00	0.00	0.15	0.00	0.99	0.11	0.80	0.70
	Daily Totals (hrs/day)			0.00	1.56	1.90	5.11	2.53	7.64	

Appendix D: Specifications of Measurement Tools

Data Logger

- Number of inputs: 8 channels
- Recording: 200,000 events (expandable)
- Measuring Input : Temperature and humidity sensors
- Resolution: 0.1ºC and < 0.5 % RH
- Input resistance : 4.15 + 0.15 M
- Measurement error: ± 0.2% (± 0.8 % max for temperature and ± 2% for humidity)
- Configuration & preset without PC / Displayed as data or graph on MS Excel
- Software: displayed as data or graph on MS Excel
- Power supply : 220 Vac/50 Hz 0.4 watt or 12Vdc/25mA
- Logging Rate (Sample Interval) : 1 seconds - 60 minutes; 1 - 24 hrs (programmable)

Humidity Sensor

- Output: Interface to data logger
- Measurement range: 10 - 100 %RH
- Measurement error: ± 2 %
- Operating temperature : 0 - 70ºC
- Supply : 12 Vdc/20mA
- Output cable length: 2 m (max)
- Response time: 60 sec

Air & Surface Temperature Sensor

- Output: Pulse modulated, Interface to data logger
- Measurement range: -40 to 125ºC
- Measurement error: < ± 0.5ºC @ 0 to 50ºC
- Measurement error: < ± 1ºC @ 0 to 100ºC
- Resolution: 0.1ºC
- Storage temperature: -50 to +150ºC
- Supply: 5Vdc/200 microampere
- Response time: 11.2 sec (moving air with speed of 3.5 m/sec)

Outputs

1. International Publications

Praditsmanont, A. & Chungpaibulpatana, S., *Performance Analysis of the Building Envelope: A case study of the Main Hall, Shinawatra University*. Energy and Buildings (to be submitted)

2. Research Benefits

The urbanization in Thailand has been developed steadily in recent years which results in the significant increase of the large number of commercial buildings in Bangkok and over Thailand. These building are fully air-conditioned and consume energy immensely. With the high oil price and the shortage of energy resources, the energy conservation in buildings becomes necessity. Energy conservation in each and every building can produce a significant impact on the reduction of energy import and production in national level. A few benefits on building energy conservation from this research are suggested as follows:

- The simulation program in this study can be used to assess the energy performance of the envelope in other buildings, and the results of the analysis could be taken as a guideline for improvement the performance of building envelope. The program could also be utilized in both the design of new buildings and the improvement of existing buildings in the conservation of energy.
- The results of this research study not only reconfirm the advantage of using this high energy efficient envelope to conserve the energy but also suggest the preferable return financially for the investment and operating costs of the building. As the energy costs constantly increase, the payback period will get even shorter and the cost advantages will be even higher. These results could be used by the government to promote the benefits of utilizing the energy efficient materials as a common building envelope, and to encourage the building industries to develop and manufacture high energy efficient materials for building envelope.
- This research clearly supports the improvement of the building energy code in Energy Conservation Promotion Act (ECP Act) for new and existing buildings. The new energy code for OTTV could be implemented for new buildings on a mandatory basis, and for existing buildings on voluntary basis.